The Meteoritical Society

Meteoritics & Planetary Science 43, Nr 9, 1439–1464 (2008)
Abstract available online at http://meteoritics.org

Ca,Al-rich inclusions in Rumuruti (R) chondrites

Surya Snata ROUT and Addi BISCHOFF*

Institut für Planetologie, Wilhelm-Klemm-Str. 10, 48149 Münster, Germany
*Corresponding author. E-mail address: bischoa@uni-muenster.de

(Received 20 November 2007; revision accepted 29 March 2008)

Abstract–Rumuruti chondrites (R chondrites) constitute a well-characterized chondrite group different from carbonaceous, ordinary, and enstatite chondrites. Many of these meteorites are breccias containing primitive type 3 fragments as well as fragments of higher petrologic type. Ca,Al-rich inclusions (CAIs) occur within all lithologies. Here, we present the results of our search for and analysis of Al-rich objects in Rumuruti chondrites.

We studied 20 R chondrites and found 126 Ca,Al-rich objects (101 CAIs, 19 Al-rich chondrules, and 6 spinel-rich fragments). Based on mineralogical characterization and analysis by SEM and electron microprobe, the inclusions can be grouped into six different types: (1) simple concentric spinel-rich inclusions (42), (2) fassaite-rich spherules, (3) complex spinel-rich CAIs (53), (4) complex diopside-rich inclusions, (5) Al-rich chondrules, and (6) Al-rich (spinel-rich) fragments. The simple concentric and complex spinel-rich CAIs have abundant spinel and, based on the presence or absence of different major phases (fassaite, hibonite, Na,Al-(Cl)-rich alteration products), can be subdivided into several subgroups.

Although there are some similarities between CAIs from R chondrites and inclusions from other chondrite groups with respect to their mineral assemblages, abundance, and size, the overall assemblage of CAIs is distinct to the R-chondrite group. Some Ca,Al-rich inclusions appear to be primitive (e.g., low FeO-contents in spinel, low abundances of Na,Al-(Cl)-rich alteration products; abundant perovskite), whereas others were highly altered by nebular and/or parent body processes (e.g., high concentrations of FeO and ZnO in spinel, ilmenite instead of perovskite, abundant Na,Al-(Cl)-rich alteration products). There is complete absence of grossite and melilite, which are common in CAIs from most other groups. CAIs from equilibrated R-chondrite lithologies have abundant secondary Ab-rich plagioclase (oligoclase) and differ from those in unequilibrated type 3 lithologies which have nepheline and sodalite instead.

INTRODUCTION

The R chondrites are known as a relatively new, well-characterized chondrite group different from carbonaceous, ordinary, and enstatite chondrites (e.g., Bischoff et al. 1994; Rubin and Kallemeyn 1994; Schulze et al. 1994; Kallemeyn et al. 1996). They are named after the Rumuruti meteorite, the first and so far the only R-chondrite fall (Schulze and Otto 1993; Schulze et al. 1994). The first R chondrite to be characterized, Carlisle Lakes, was found in Australia in 1977 (Binns and Pooley 1979; Rubin and Kallemeyn 1989). About half of the R chondrites are regolith breccias showing the typical light/dark structure and having solar wind-implanted rare gases (Weber and Schultz 1995; Bischoff and Schultz 2004; Bischoff et al. 2006). These meteorites contain unequilibrated, type 3 fragments (Bischoff et al. 1998; Bischoff 2000) and clasts metamorphosed to various degrees, and should be considered as R3–5 or R3–6 breccias (e.g., Bischoff et al. 1994; Schulze et al. 1994; Kallemeyn et al. 1996). Unequilibrated chondritic components have been reported from many R chondrites (e.g., Weisberg et al. [1991; their Fig. 1]; Schulze et al. [1994; their Fig. 5]; Bischoff et al. [1994; their Fig. 5]; Rubin and Kallemeyn [1994; their Fig. 4a]). Jäckel et al. (1996) reported several type 3 clasts in Dar al Gani 013 having a perfect chondritic texture. Unequilibrated R chondrite lithologies can easily be recognized in backscattered electron images in having a well-preserved chondritic texture and variable abundances of zoned olivines (mainly in chondrules), which generally are richer in Fo contents ($Fo_{60–100}$) than the olivine in equilibrated R chondrite lithologies (~Fo_{60}). For further details see Bischoff (2000). The aim of this study is to search for and identify Ca,Al-rich inclusions within these primitive (type 3) and other fragments from Rumuruti (R) chondrites to

© The Meteoritical Society, 2008. Printed in USA.

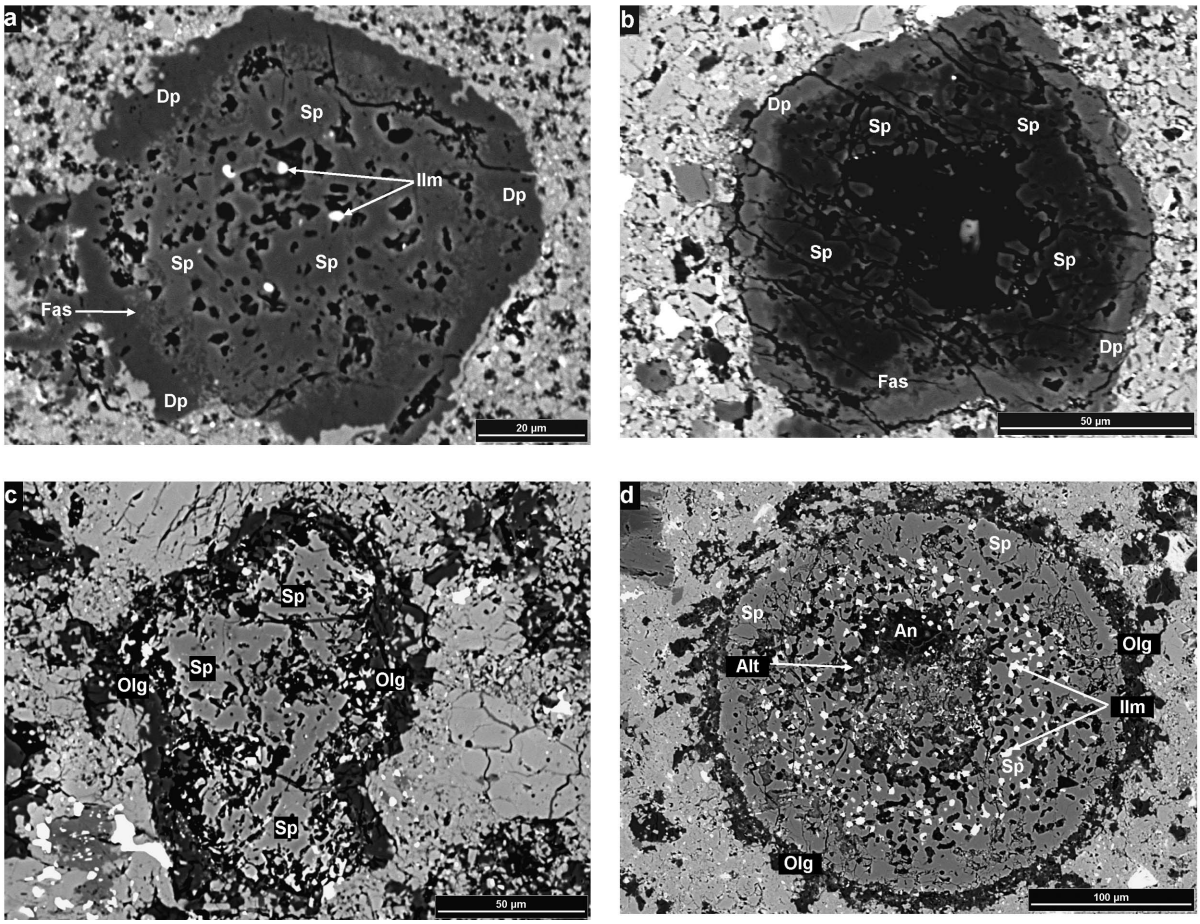


Fig. 1. BSE images of typical simple concentric spinel-rich inclusions. a) CAI 2446/112 (from NWA 2446) has a uniform monomineralic rim of Al-diopside (Dp). There is a thin, barely visible fassaitic (Fas) rim below the Al-diopside rim enclosing the spinel (Sp). b) inclusion 1476/83 (NWA 1476) is rimmed by a layer of diopside (Dp) followed by a very thin rim of fassaite (Fas). The spinels (Sp) have very low Fe contents. c) Inclusion 1478/12 (NWA 1478) and d) inclusion 1566/32 (NWA 1566) are from metamorphosed R-chondrite host lithologies showing in the rim areas abundant oligoclase (Olg) (dark grey) instead of nepheline. Tiny ilmenites (Ilm), white spots, occur within the spinel-rich cores (Sp). Inclusion 1566/32 also has probably some amount of terrestrial alteration products as indicated by the presence of some sulfates (Alt) and minor amounts of anorthite (An).

characterize CAIs in R chondrites and to compare these CAIs with those of other chondrite groups. In addition, we also searched for CAIs in equilibrated (metamorphosed) lithologies of these meteorites.

Previously only eleven Al-rich objects have been described from R chondrites (Russell 1998; Berlin 2003; Bischoff and Srinivasan 2003). Here we present the results of our search and analysis of Al-rich objects in 20 Rumuruti chondrites. Preliminary data have been published by Rout and Bischoff (2007).

SAMPLES AND ANALYTICAL PROCEDURES

Polished thin and thick sections from Rumuruti (Rumuruti, Ru), Dar al Gani (DaG) 013 (PL95141, PL96218), DaG 417 (PL07035), Hughes 030 (PL98092, PL98016, PL98092), Northwest Africa (NWA) 053 (PL00033), NWA 753 (PL06079, PL01124 and three polished thick sections) NWA 755 (PL01125, PL01078), NWA 3364 (PL05191), NWA 1477 (PL02155, PL07072), NWA 2446 (PL041577, PL07040, PL07041, PL072091), Sahara 99531 (PL07071, PL99076), Sahara 99537 (PL99077; PL07070), NWA 1476 (PL02154, PL07042, PL07043), NWA 1478 (PL02156), NWA 1471 (PL02149), NWA 1566 (PL02213), NWA 1472 (PL02150), Hammadah al Hamra (HaH) 119 (PL07037), Acfer 91217 (PL92272), and Dhofar 1223 (PL04070, PL07039) were studied by optical microscopy in transmitted and reflected light. A JEOL 840A scanning electron microscope (SEM) was used to search for the CAIs, to resolve the fine-grained texture of these Al-rich objects, and to identify phases with a Pentafet detector (Oxford Instruments) for energy dispersive (EDS) semiquantitative elemental analysis using the INCA analytical program provided by Oxford Instruments. Quantitative mineral analyses were obtained using a JEOL 8900 electron microprobe operated at 15 kV and a probe current of 15 nA. Natural and synthetic standards of well-known compositions were used as standards. These are jadeite (Na), sanidine (K), diopside (Ca),

Table 1. Characterization and listing of the meteorite samples and inclusions studied.

Meteorite	Class	Type 3[a]	Ref.	Inclusion numbers[b]
Rumuruti	R3–5	Rare	1, 2	RA/21 (3), RA/43A(1), RA/43B(1), RA/53 (3), RA/911(1), RB/81(5)
Hammadah al Hamra 119	R4		3	None
Sahara 99531	R3–5	Rare	4	ShrB/41 (1)
Sahara 99537	R3–6	Rare	4	None
Acfer 217	R3–5	Rare	5	Afr/4L (3), Afr/61 (5), Afr/111 (5)
Dar al Gani 013	R3.5–6	Few	6, 7	D013/23 (1), D013/24 (3), D013/44 (1), D013B/15 (1), D013B/35 (1), D013B/65 (3), D013B/71 (5), D013B/88 (5), D013B/118 (1), D013B/119 (3), D013B/144 (5), D013B/183 (5)
Dar al Gani 417	R3–4	Few	8	D417/43 (3), D417/61 (5)
Hughes 030	R3–6	Few	9	H030/22 (3), H030/2L (6), H030/L (1)
Dhofar1223	R3		10	Dfr/23 (2), Dfr/53 (3), Dfr/75 (3), DfrB/2L (1), DfrB/12 (5), DfrB/32 (5)
NWA 053	R4	No	11	None
NWA 753	R3.9[c]		11	753/1L (3), 753/22 (3), 753/24 (3), 753/31A (3), 753/31B (3), 753/35 (3), 753/37 (3), 753/42 (3), 753/44 (3), 753/46 (3), 753/4L (3), 753/52 (3), 753/6L (3), 753/73 (1), 753/93 (3), 753/95 (3), 753/102 (1), 753/104A (1), 753/104B (1), 753/111 (1), 753/116A (1), 753/116B (1), 753/116C (3), 753/11L (1), 753/12LA (3), 753/12LB (6), 753/131 (3), 753/143 (1), 753/154 (1), 753B/13 (1), 753B/14 (2), 753B/23 (6), 753B/33 (3), 753B/34 (1), 753B/62 (1), 753B/6L (3), 753C/21 (5), 753C/31 (3), 753C/51 (3), 753D/54 (3), 753D/64 (3), 753D/74 (3), 753_124/21 (3), 753_124/23 (1), 753_124/12L (1), 753_124/33 (6).
NWA 755	R3.7		11	755/13 (6), 755/13B (5), 755/31 (3), 755/33 (5).
NWA 1471	R3/4		12	1471/23 (3), 1471/3L (3)
NWA 1472	R3/4		12	1472/12 (1), 1472/15 (3), 1472/56 (1), 1472/117 (3), 1472/119 (3), 1472/1711 (3).
NWA 1476	R3[c]		12	1476/22 (5), 1476/74 (5), 1476/83 (1), 1476/124 (2), 1476B/12 (3), 1476C/54 (3), 1476C/62A (1), 1476C/62B (3), 1476C/8L (1), 1476C/101 (3), 1476C/102 (3).
NWA 1477	R3[c]		12	None
NWA 1478	R3		12	1478/12 (1), 1478/35 (3)
NWA 1566	R3.8		12	1566/32 (1)
NWA 2446	R3[c]			2446/12 (3), 2446/23 (1), 2446/31A (4), 2446/31B (3), 2446/33 (1), 2446/63 (4), 2446/71A (3), 2446/71B (5), 2446/84 (1), 2446/85 (5), 2446/112 (1), 2446/122A (3), 2446/122B (4), 2446/L (1), 2446B/1L (3), 2446B/54 (3), 2446B/5L (6), 2446B/8L (1), 2446B/9L (5), 2446C/51 (5), 2446D/2L (1), 2446D/33A (3), 2446D/33B (3), 2446D/41 (3), 2446D/71 (5).
NWA 3364	R3–5	Rare	13	None

[a]Indicates the abundance of type 3 lithologies in breccias; Ref = References: (1) Schulze et al. 1994; (2) Berlin 2003; (3) Weber et al. 1997; (4) Grossman 2000; (5) Bischoff et al. 1994; (6) Jäckel et al. 1996; (7) Grossman 1996; (8) Grossman 1999; (9) Grossman 1998; (10) Russell et al. 2005; (11) Grossman and Zipfel 2001; (12) Russell et al. 2003; (13) Connolly et al. 2006.

[b]The number in brackets after the inclusion number indicates the inclusion type: (1) Simple concentric spinel-rich CAIs, (2) Fassaite-rich spherules, (3) Complex spinel-rich CAIs, (4) Complex diopside-rich inclusions, (5) Al-rich chondrules, and (6) Al-rich (spinel-rich) fragments.

[c]Some R3 chondrites are breccias: NWA 753, NWA 1476, NWA 1477, NWA 2446.

apatite (P), V-metal (V), disthen (Al), fayalite (Fe), chromite (Cr), flourite (F), NiO (Ni), hypersthene (Si), forsterite (Mg), rhodonite (Mn), rutile (Ti), tugtupite (Cl), scapolite (S), and willemite (Zn). The matrix corrections were made by the $\Phi\rho(z)$ procedure of Armstrong (1991).

MINERALOGY, PETROLOGY, AND CLASSIFICATION OF Ca,Al-RICH INCLUSIONS

Using the analytical procedures described above, 126 Al-rich objects (101 CAIs, 19 Al-rich chondrules, and 6 Al-rich fragments) were found (Table 1) and studied within 20 R chondrites. In general, (a) most of the inclusions and fragments are very small, <50–100 μm, with the largest being 600 × 200 μm in size. (b) They are rare; probably slightly more abundant than CAIs in ordinary and enstatite chondrites (e.g., Bischoff and Keil 1983a, 1983b, 1983c; 1984; Bischoff et al. 1984; Fagan et al. 2000). (c) There is a marked difference in mineralogy between the CAIs in the R3 chondrites (or breccia fragments of type 3) compared with inclusions of types R4–R6 (or breccia fragments of types 4–6). (d) Melilite, an abundant phase in CAIs of many other chondrite groups (e.g., Grossman et al. 1975; MacPherson and Grossman 1979; MacPherson et al. 1988; Brearley and Jones 1998, and references therein) and grossite (abundant in CR and CH chondrites; e.g., Bischoff et al. 1993a, 1993b; Weber and Bischoff 1994) were not found in refractory inclusions from R chondrites.

Based on the dominant mineral phases present and their textural characteristics, we divided the Al-rich objects into six

different groups: (1) simple concentric spinel-rich CAIs, (2) fassaite-rich spherules, (3) complex spinel-rich CAIs, (4) complex diopside-rich inclusions, (5) Al-rich chondrules, and (6) Al-rich fragments (Table 1). According to the definition of MacPherson and Davis (1994), who defined inclusions in the CM chondrite Mighei as "simple inclusions," in this paper similar inclusions in R chondrites are defined as "simple concentric inclusions," which have a single, rounded or ovoid, spinel-rich core concentrically rimmed by one or more mineral layers. On the other hand "complex inclusion" indicates that the overall shape of the inclusion does not conform to a spherical or simple ovoid object. The latter are irregularly shaped and sometimes have highly convoluted margins.

Simple Concentric Spinel-Rich Inclusions

These are dominated by spinel and have compact textures. Most have a single- or double-layered rim sequence. The single-layered rims are composed only of Al-diopside, whereas the double-layered rims have Al-diopside along with fassaite or olivine, unlike the Wark-Lovering rims, which typically consist of some more mineral layers and often include spinel and secondary alteration phases (Wark and Lovering 1977).

Taking into account the presence of other primary mineral phases, along with spinel, we divided the simple concentric spinel-rich CAIs into four sub-groups: (a) simple concentric spinel-rich CAIs, (b) simple concentric spinel- and hibonite-rich CAIs, (c) simple concentric spinel- and fassaite-rich CAIs, (d) simple concentric spinel- and Na,Al alteration product-rich CAIs.

Simple Concentric Spinel-Rich CAIs

A total of 14 were studied (Fig. 1). Their sizes range from ~250 μm (Fig. 1d) to ~40 μm in apparent diameter. As the name suggests, the primary phase is spinel, whose composition ranges from pure spinel to Fe- and Zn-bearing spinels (see below: mineral compositions). In general, the iron component in the spinel increases with increasing petrologic type (primitive type 3 host material versus type 4 to 6 R chondrite material). Accessory mineral phases include perovskite and ilmenite. A monomineralic rim (~5 μm) of diopside or Al-diopside is almost always present, occasionally underlain by fassaite (Fig. 1). Small perovskite grains are locally associated with spinel and are transformed to ilmenites with increasing iron content of the spinel. Unlike some nodular and fluffy spinel-rich CAIs in CM meteorites (MacPherson and Davis 1994), simple concentric spinel-rich CAIs in R chondrites are compact (Fig. 1) and uniform, some with minor alteration. Alteration products occur in one inclusion between the Al-diopside rim and the spinel-rich core; in other cases they are mostly distributed throughout the spinel. Some spinels have very low FeO contents (~0.5–1 wt%) and these CAIs belong to the least altered found in R chondrites (Fig. 1b). In CAIs from metamorphosed host

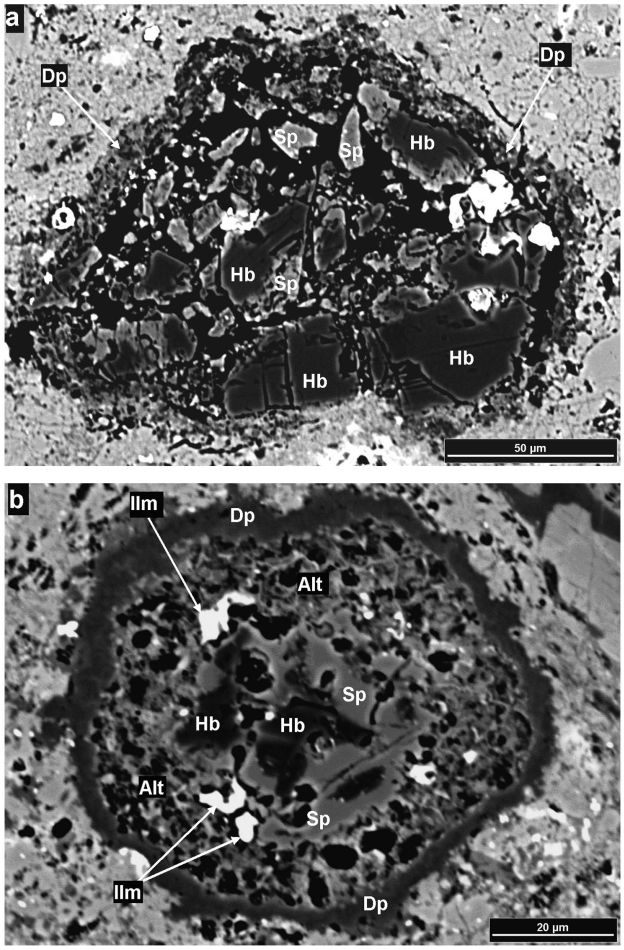


Fig. 2. BSE images of simple concentric spinel- and hibonite-rich CAIs in R chondrites. a) Inclusion H030/L (Hughes 030) has abundant hibonite (Hb) and spinel (Sp). b) 2446B/8L (NWA 2446) has abundant spinel (Sp) along with hibonite (Hb) and alteration products (Alt). Both inclusions are rimmed by diopside (Dp) and have high porosity (black areas). The white spots in (a) are Au-contamination remnants from Au-coating, those in (b) are ilmenite (Ilm).

lithologies, distinct oligoclase rims (~Ab_{85}) are present (Figs. 1c and 1d). The rim oligoclase is similar in composition to that of typical R4–R6 chondrite matrix oligoclase and is most probably a metamorphic product. One of the CAIs in a metamorphosed fragment shows a high abundance of ilmenite with an unusual "concentric" distribution (Fig. 1d).

Simple Concentric Spinel- and Hibonite-Rich CAIs

Only three such inclusions were found and studied. One has a very high proportion of hibonite (Fig. 2a) (Bischoff and Srinivasan 2003), whereas the other two are dominated by spinel and alteration products (Fig. 2b). In the latter two CAIs the hibonite grains are enclosed in spinel (Fig. 2b). All three CAIs have diopsidic rims, which is very fine-grained in case of CAI H030/L. Ilmenite occurs as a minor accessory phase and some sulfide-rich alteration products are also abundant in 2446B/8L, which may be due to terrestrial weathering. These CAIs are very rare in R chondrites.

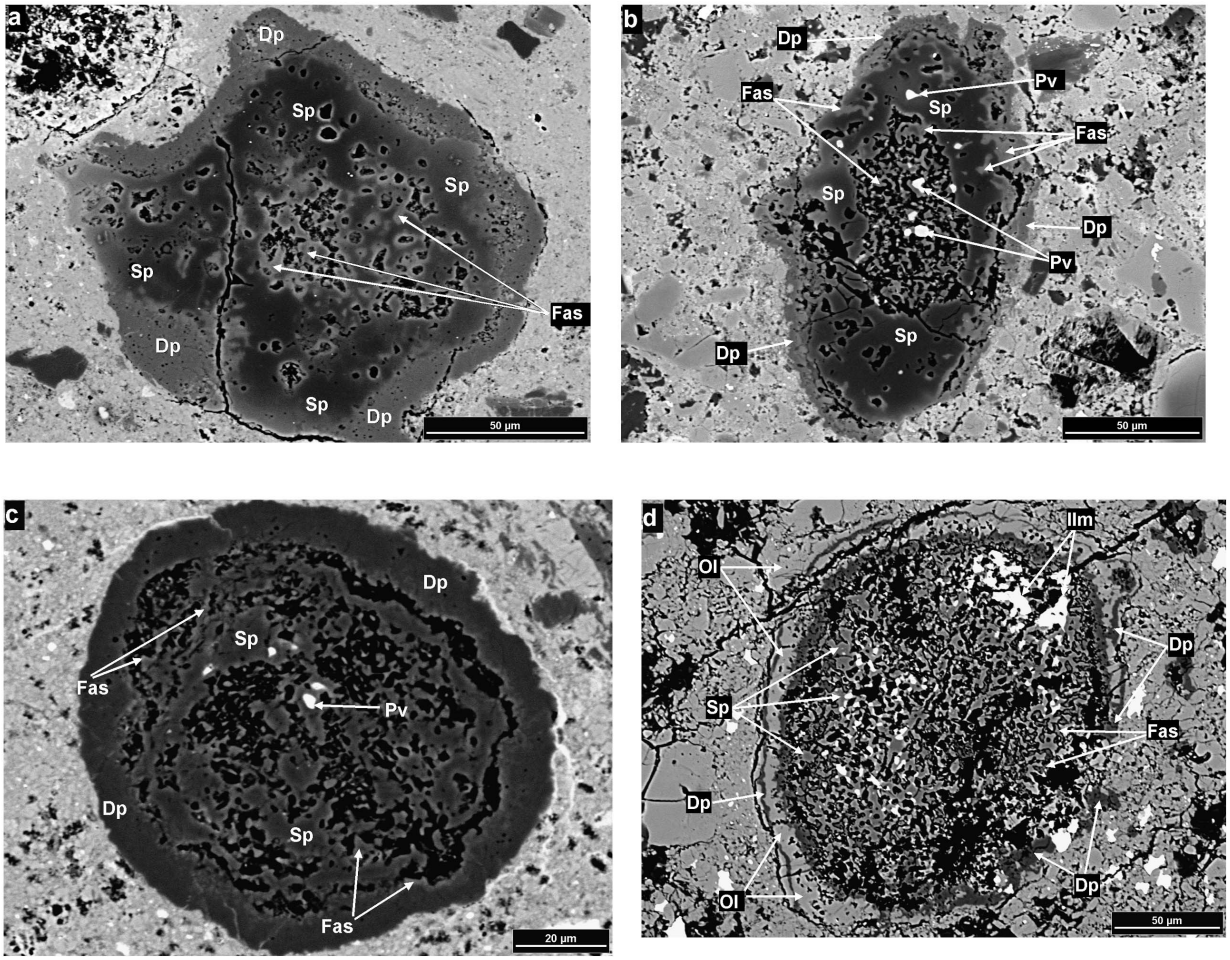


Fig. 3. BSE images of simple concentric spinel- and fassaite-rich CAIs. a) Inclusion D013/44 (Dar al Gani 013). b) Ca,Al-rich inclusion D013B/118 (Dar al Gani 013). c) Inclusion 2446/84 (NWA 2446). d) Inclusion 753_124/12L (NWA 753); Fassaite (Fas) is normally intergrown with spinel (Sp). Spinels in (a), (b), and (c) are low in FeO (dark grey), whereas spinel in (d) is rich in FeO (light grey). The CAIs are rimmed by a uniform single layer of diopside (a, c), or by several layers consisting of Al-diopside (Dp) and fassaite (Fas; b) or olivine (Ol) intermixed with diopside (Dp; d). The white phases within the inclusions are either perovskite (Pv) or ilmenites (Ilm).

Simple Concentric Spinel- and Fassaite-Rich CAIs

Thirteen were identified in type 3 R chondrites as well as in higher petrologic types. They range in size from 50 to 200 µm in apparent diameter. Texturally they are very similar to the simple concentric spinel-rich CAIs, but with abundant fassaite. Spinels of CAIs found in lithologies of lower petrologic types have very low iron contents, as low as 0.5–1 wt% (Fig. 3b), but CAIs from strongly metamorphosed lithologies have spinels with high FeO and ZnO-contents of ~>20 wt% (Fig. 3d) and ~2–4 wt%, respectively. Inclusion D013B/118 (Fig. 3b) is the least-altered among the simple concentric spinel- and fassaite-rich inclusions. Minor perovskite is present in CAIs having Fe-poor spinels, but is increasingly transformed to ilmenite as the iron content in spinel increases. These CAIs are mostly rimmed by uniform single layers of diopside (Figs. 3a and 3c), but in some cases by several layers of Al-diopside and fassaite (Fig. 3b) or diopside and olivine (Fig. 3d). Fassaite is typically intergrown with spinel (Fig. 3a).

Simple Concentric Spinel- and Na,Al Alteration Product-Rich CAIs

These 12 CAIs are very small, with ~70% ≤50 µm in apparent diameter, and the largest being ~150 µm in diameter. In general they texturally resemble the simple concentric spinel-rich and simple concentric spinel- and fassaite-rich CAIs, but there are many exceptions. Besides the high modal abundances of spinel, these inclusions have significant abundances of Na-, Al- and/or Cl-rich constituents, which we refer to as "Na,Al-rich alteration products." In unequilibrated lithologies of R chondrites, this product consists of nepheline and/or sodalite or mixtures of both (Figs. 4a and 4b), apparently filling all pores within the inclusions, whereas in CAIs from type R4–R6 lithologies, these components are partially to completely replaced by oligoclase (~Ab_{85}; Fig. 4d). As stated earlier for other types of inclusions, the spinels also show a similar trend: increasing FeO content with increase in metamorphic type. None of the CAIs contain any accessory perovskite, but few grains of ilmenite are present in some.

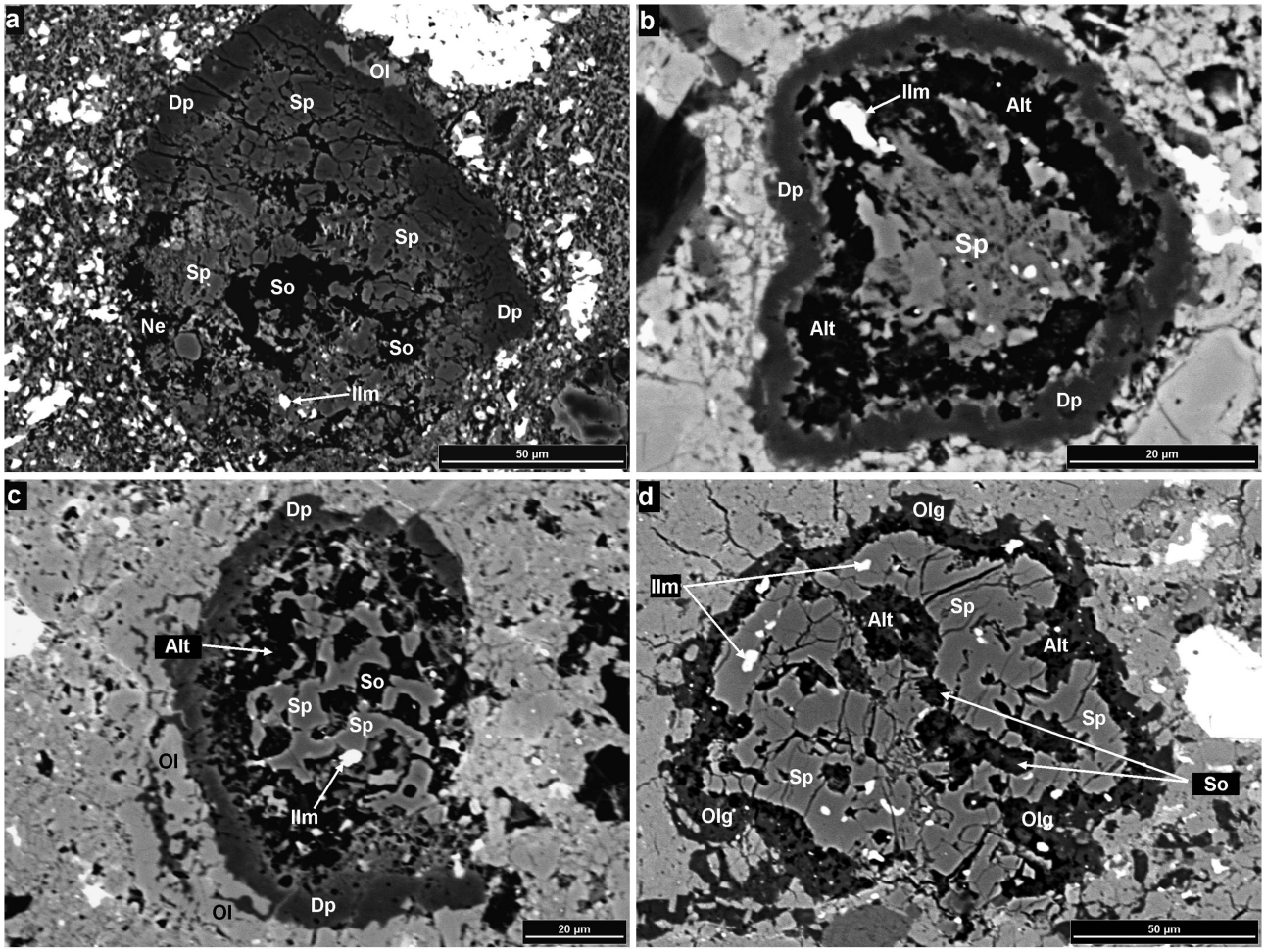


Fig. 4. BSE images of simple concentric spinel- and Na,Al alteration product-rich CAIs. a) Inclusion RA/43 (Rumuruti). b) CAI 753/104A (NWA 753). c) Inclusion 1472/56 (NWA 1472). d) Inclusion ShrB/41 (Sahara 99531). The main phase of the inclusions is spinel (Sp, grey). The Na,Al alteration products (Alt) fill most of the pores (dark grey to black). This material is mainly nepheline (Ne) and/or sodalite (So) or mixtures of both (b, c, d); in metamorphosed CAIs these components are partially to almost completely replaced by oligoclase (Olg; d). White spots are ilmenite (Ilm). The inclusions are rimmed by diopside (Dp; a, b) or a mixture of diopside (Dp) and olivine (Ol; c) or oligoclase (Olg; d).

These inclusions show more complex rimming than those discussed before. Many inclusions have a rim showing a layer of intermixed olivine + diopside above the diopside rim (Fig. 4c). Others have a monomineralic rim of diopside or oligoclase (Fig. 4d). One of the inclusions does not show any rimming and has a different mineral assemblage, with high nepheline and olivine (~$Fa_{37–38}$) contents, minor oligoclase replacing nepheline and low spinel, very unlike the other inclusions which have spinel as the primary phase. Simple concentric spinel- and Na,Al alteration product-rich CAIs from higher petrologic lithologies (having oligoclase also within the olivine-rich matrix; type R4–R6) have a rim of oligoclase (~Ab_{80}) (Fig. 4d).

Fassaite-Rich Spherules

Three inclusions were studied: they are rich in fassaite and their textures suggest that they solidified from melt droplets. One inclusion (Fig. 5a) has hibonite laths, and the other two have spinel as the dominant phase after fassaite. One (Fig. 5b) also has skeletal laths of olivine with varying Fa content and abundant accessory Cr, Fe, Al, Ti-rich oxides. Based on the texture of the grains both olivines appear to have formed in situ. Spinels have high FeO and ZnO (~20–24 and 2 wt%, respectively) and euhedral textures (Fig. 5b), which suggests crystallization from a melt. Inclusion 1476/124 (Fig. 5a) does not have a uniform fassaitic groundmass, but an intergrowth of diopside and fassaite.

Complex Spinel-Rich CAIs

Like the simple concentric spinel-rich CAIs, this group also has spinel as the most abundant phase, but the texture is completely different. The spinel-rich CAIs have complex textures, and some have amoeboid shapes. Based on the presence of other dominant mineral phases, we divided the 53 inclusions into four subgroups: (a) complex spinel- and hibonite-rich CAIs, (b) complex spinel- and plagioclase-rich

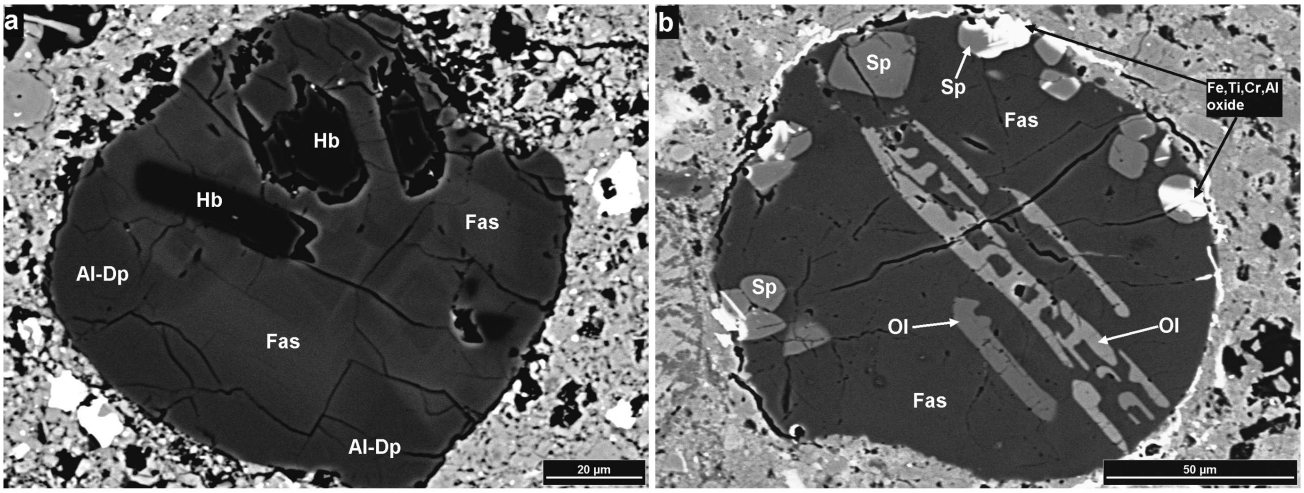


Fig. 5. BSE images of fassaite-rich spherules. (a) 1476/124 (NWA 1476), (b) Dfr/23 (Dhofar 1223). Both are devoid of rims. Groundmass in (a) shows two phases–fassaite (Fas; light) and Al-diopside (Al-Dp; dark). Three distinct hibonite (Hb) laths are visible. Euhedral spinels (Sp) and laths of olivine (Ol) are seen within fassaite in (b). The olivine laths in (b) have varying Fe contents (light and dark grey grains have ~Fa_{28} and ~Fa_{39}, respectively), and minor Fe, Ti, Cr, Al-rich oxides are present as white phases.

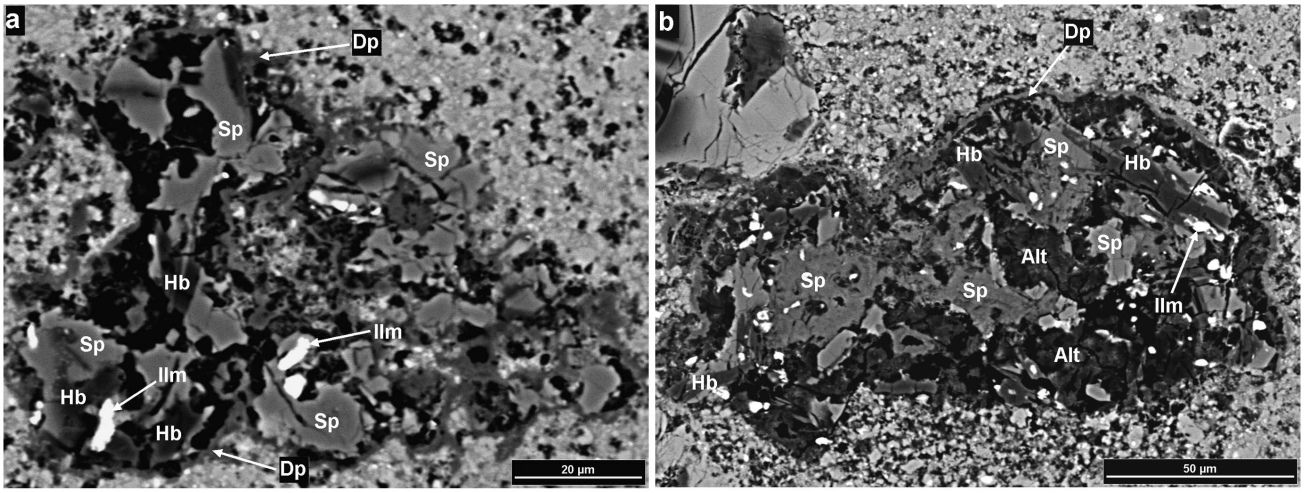


Fig. 6. BSE images of complex spinel- and hibonite-rich CAIs. a) Inclusion 2446/122A (NWA 2446), b) Inclusion 2446/12 (NWA 2446). They contain laths of hibonite (Hb) and tiny ilmenites (Ilm; white) mainly enclosed in spinel (Sp). Dark grey to black areas are either pores or Al, Si-rich alteration products (Alt). Both inclusions have thin rims of diopside (Dp).

CAIs, (c) complex spinel- and fassaite-rich CAIs, and (d) complex spinel- and Na,Al alteration product-rich CAIs. The latter subgroup also contains one complex spinel-rich inclusion with only a moderate abundance of alteration products (see below).

Complex Spinel- and Hibonite-Rich CAIs

These inclusions are very rare, similar in abundance to the simple concentric spinel- and hibonite-rich inclusions, and only two could be found. The largest is ~150 × 75 µm in apparent size and has a very complex texture. Both inclusions have very thin rims of diopside and numerous accessory ilmenite grains. Spinel in both is Fe-rich. The inclusion in Fig. 6b also has abundant Al, Si-rich alteration products, which may have replaced melilite or anorthite.

Complex Spinel- and Plagioclase-Rich CAIs

These are the most abundant variety of CAIs in Rumuruti chondrites, and 27 were studied. Typical minerals are spinel, hercynite, oligoclase (~$Ab_{80–85}$), anorthite, fassaite, and diopside. Spinel-anorthite-rich inclusions were found in type 3 lithologies, whereas spinel-oligoclase-rich inclusions, which consist of about 70% spinel and oligoclase, were found in metamorphosed R chondrite components (Fig. 7a). Some inclusions have up to 80 vol% oligoclase, which has probably completely replaced the nepheline/sodalite assemblage that may have been present prior to metamorphism and secondary parent body alteration.

Anorthite, when present, is mostly primary and may be only partly replaced by secondary oligoclase in metamorphosed chondrites and fragments (Figs. 7b and 7d).

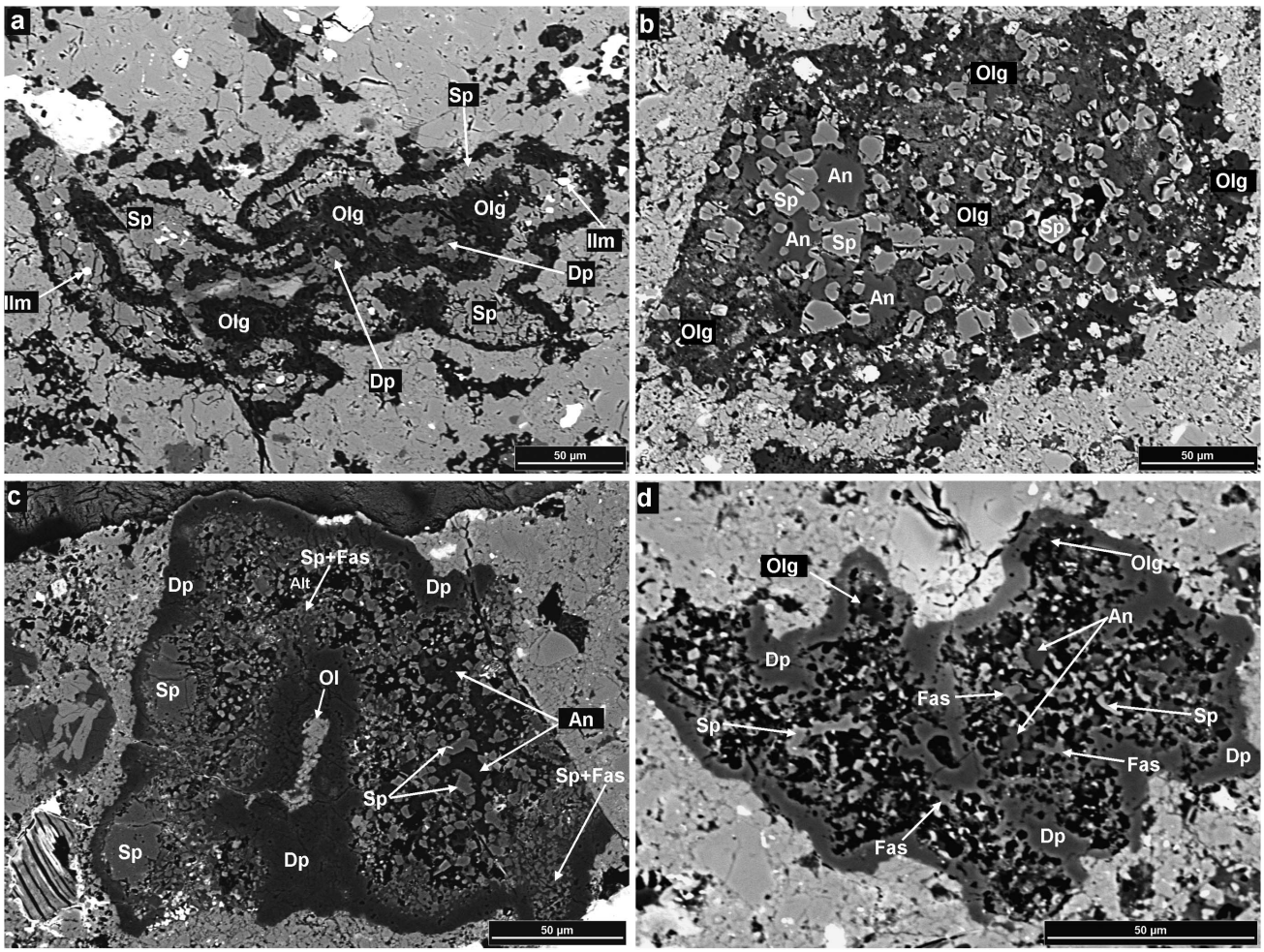


Fig. 7. BSE images of complex spinel- and plagioclase-rich CAIs. a) CAI D417/43 (Dar al Gani 417); this metamorphosed inclusion has abundant oligoclase (Olg) occurring in the core and at the rim. Abundant spinel (Sp) grains are arranged along the rim and minor diopside (Dp) is also present within the oligoclase. Some ilmenite (Ilm) grains are scattered within the inclusion. A micro-fault is visible in the left part of the image. b) 753C/51 (NWA 753); note that this metamorphosed inclusion does not have a rim. Oligoclase (Olg) is abundant and seems to replace anorthite (An). Euhedral grains of spinel (Sp) are spread throughout the inclusion. c) Inclusion 753/6L (NWA 753) is from the type 3 lithology and exhibits no alteration of anorthite (An). Just below the rim of diopside (Dp), there is a complex mixture of spinel and fassaite (Sp + Fas). Some minor Na,Al-rich alteration product (Alt) is also present (dark spots) and some olivine (Ol) grains are also embedded within the diopsidic rim, which are probably matrix olivines filling indentations of the irregularly shaped CAI. d) CAI 1472/1711 (NWA 1472) is from a metamorphosed lithology and has a diopsidic (Dp) rim which is not seen in most of the CAIs from metamorphosed lithologies. Small fassaite (Fas) grains are present along with spinel (Sp), anorthite (An), and oligoclase (Olg), which seems to replace anorthite.

Anorthite in type 3 lithologies is not affected by severe secondary processes (Fig. 7c). Most inclusions (Figs. 7a, 7c, and 7d) have a complex and irregular shape, very similar to CAIs in other chondrite classes. CAIs in metamorphosed lithologies are often devoid of rims (Fig. 7b).

Complex Spinel- and Fassaite-Rich CAIs

Eighteen complex spinel-rich inclusions have abundant fassaite and occasionally Na,Al-rich alteration products. The largest has an apparent size of ~600 µm × 200 µm (Fig. 8b), which is also the largest CAI of all studied within the R chondrites. Most appear to be a loose aggregate of grains, as inferred from their irregularly shaped, complex texture and fluffy appearance.

Na,Al-rich alteration products occur in minor abundance in several CAIs, except for inclusion Dfr/53 (Fig. 8b), which has abundant alteration products rich in Na, Al, and Cl. Spinel and fassaite are always intricately related, and most of the CAIs have complex intergrowths of both phases (Figs. 8a, 8c, and 8d). A rim of Al-diopside or pure diopside ~2–10 µm wide is present in all CAIs. The Fe content of spinel in the inclusions within the metamorphosed meteorites is higher and sometimes due to incomplete equilibration, and both Mg-rich and Mg-poor spinels are found in the same inclusion (Fig. 8c). Other accessory phases are perovskite, ilmenite, and troilite. One inclusion has abundant Al-diopside and minor fassaite (Fig. 8c).

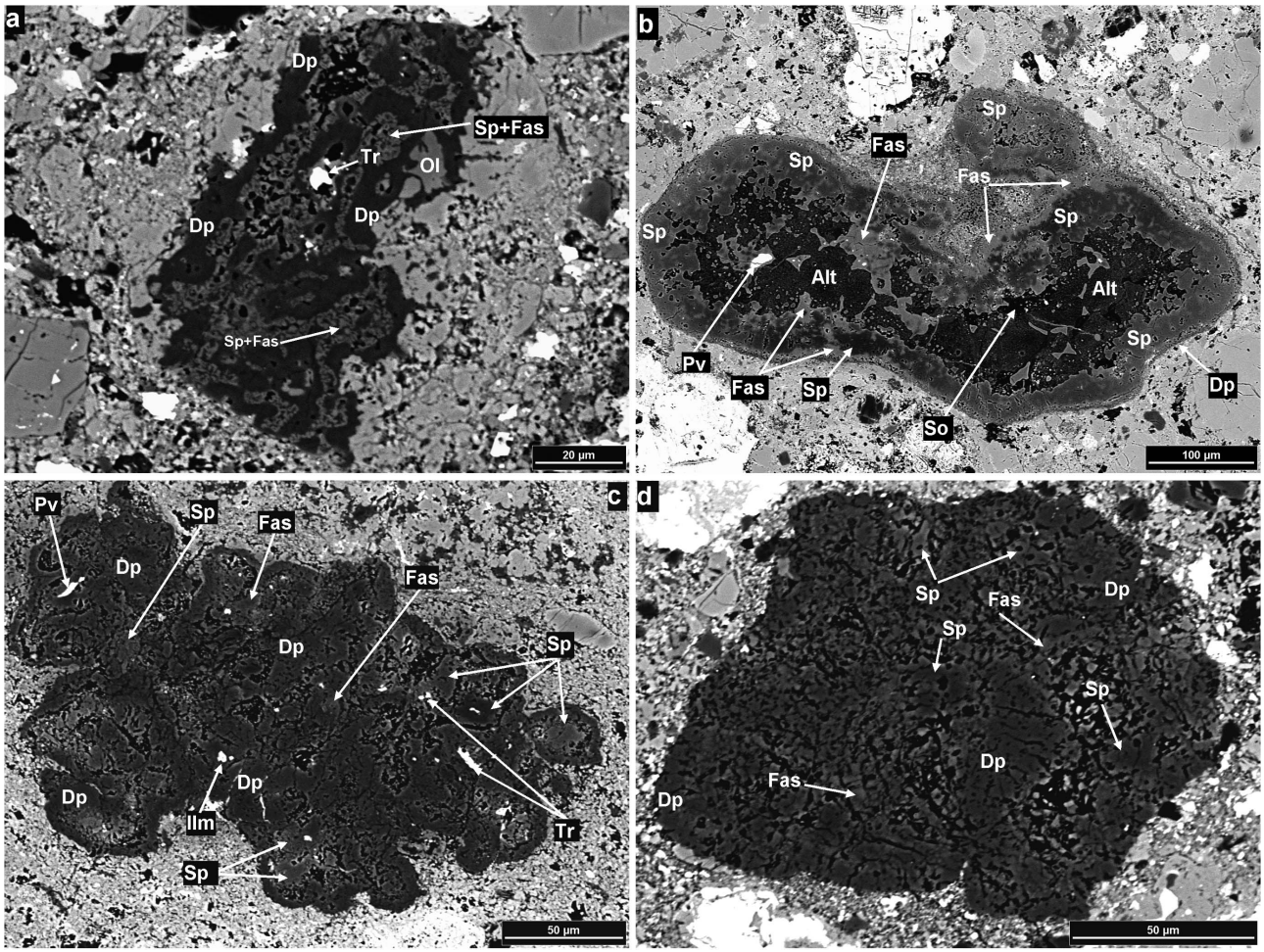


Fig. 8. BSE images of complex spinel- and fassaite-rich CAIs. a) CAI 753/46 (NWA 753) has an irregularly shaped diopside rim (Dp) enclosing a fine-grained mixture of spinel and fassaite (Sp+Fas). A large troilite (Tr) grain is found in the inclusion (white spot). b) Inclusion Dfr/53 (Dhofar 1223) has a thin rim of diopside and fassaite (Fas), spinel (Sp), and abundant Na,Al-rich alteration products (Alt) also occur. Perovskites (Pv) are scattered throughout the inclusion (white spots). Minor sodalite (So) grains are found within the altered areas. c) CAI 753D/54 (NWA 753) is present within an unequilibrated type 3 fragment. The complex diopside rim encloses few fassaites (Fas), but abundant Al-diopside (Dp) and spinel (Sp). Numerous ilmenite (Ilm), perovskite (Pv), and troilite (Tr) grains are present (white spots). d) CAI 1476C/54 (NWA 1476) consists of a complex spinel (Sp) and fassaite (Fas) mixture rimmed by Al-diopside (Dp).

Complex Spinel- and Na,Al-Alteration Product-Rich CAIs

Six such highly altered concentric inclusions were studied (Fig. 9). Most are very small, and the largest is ~300 × 75 µm in apparent size. Diopsidic rims, ~2–5 µm in width, are typically found surrounding abundant alteration products, which either are nepheline or sodalite or a mixture of both, spinel as another dominant phase, and few accessory perovskite or ilmenite grains. Within this subgroup we have also included one complex spinel-rich inclusion with only minor to moderate abundance of alteration products (Fig. 9b). This CAI is the inclusion with the lowest abundance of Na,Al-rich alteration products among all complex spinel-rich CAIs.

Complex Diopside-Rich Inclusions

This unique group has abundant diopside, and the three studied inclusions have irregularly shaped rims of diopside with a highly complex texture ranging in thickness from ~2 to ~15 µm. Minor Na,Al-rich alteration products (Fig. 10a) or spinel and fassaite (Fig. 10b) are present within the cores of nodules in one of the inclusions.

Al-Rich Chondrules

Al-rich chondrules are a well-established group of chondrules first described in studies of chondrules in ordinary chondrites (e.g., Bischoff and Keil 1983a, 1983b, 1983c, 1984; Bischoff et al. 1989). They have also been studied in enstatite and carbonaceous chondrites (e.g., Bischoff et al. 1984, 1985; Sheng et al. 1991). Krot et al. (2002) reported a group of Al-rich chondrules from CV3 chondrites and called them plagioclase-rich chondrules (PRCs). Additional studies of such objects have been reported by MacPherson and Huss (2000, 2005), Huss et al. (1997, 2001), Guan et al.

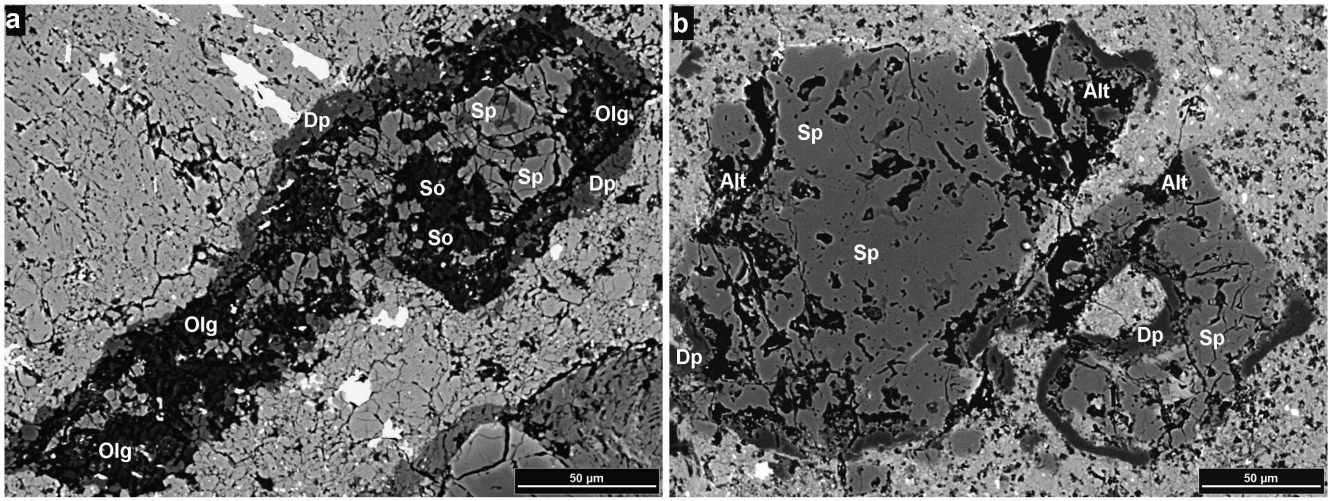


Fig. 9. a) BSE image of the complex spinel- and Na,Al-alteration product-rich CAI RA/53 (Rumuruti). It has a thin non-uniform diopside (Dp) rim and abundant sodalite (So) and spinel (Sp). Minor oligoclase (Olg) is observed replacing the nepheline. b) Complex spinel-rich CAI 2446D/33B (NWA 2446) mainly consists of spinel (Sp) and minor Na,Al-rich alteration products (Alt). It is rimmed by a thin discontinuous diopside (Dp) layer. BSE image.

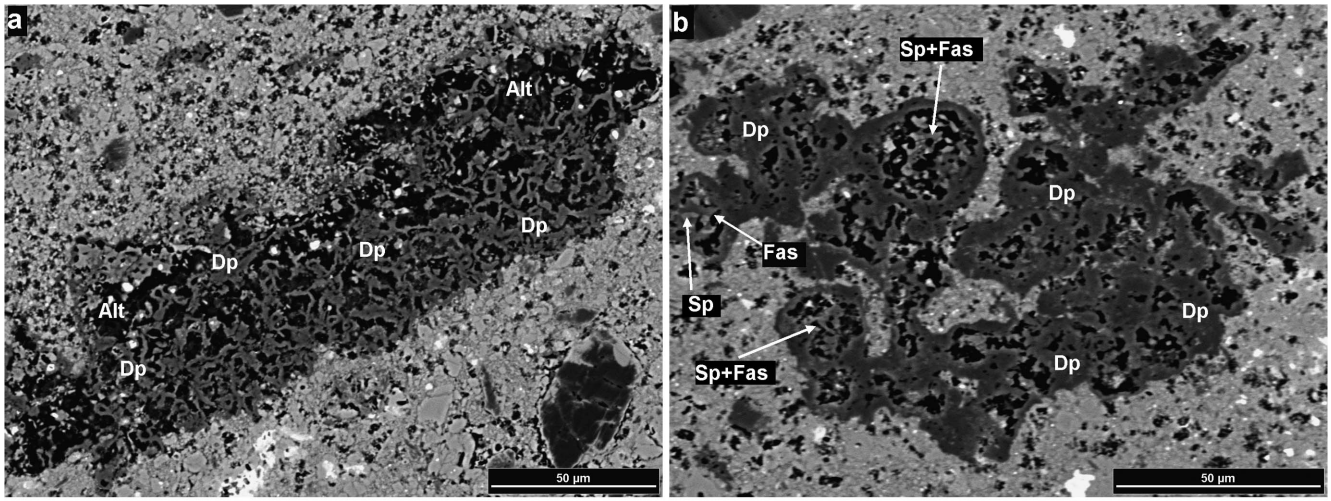


Fig. 10. BSE images of complex diopside-rich CAIs. a) 2446/31A (NWA 2446), b) 2446/122B (NWA 2446); both have extremely irregularly shaped diopside (Dp) rims. In addition, inclusion 2446/31A contains abundant alteration products (Alt; dark grey), whereas 2446/122B has spinel (Sp) and fassaite (Fas) and sometimes a very fine-grained mixture of spinel and fassaite (Sp + Fas).

(2002), Russell et al. (1997, 1998b, 2000b), Srinivasan et al. (2000), Krot et al. (2004), and Tronche et al. (2007). Here, 19 Al-rich chondrules are described from R chondrites. They vary in size, and the largest has an apparent diameter of ~550 µm (Figs. 11a and 11d). The texture and mineralogy of these chondrules are also highly variable. Some have barred textures (Fig. 11a), whereas others have textural similarities with radial pyroxene (Fig. 11b) or porphyritic chondrules (Fig. 11d). The dominant mineral phases in the chondrules are plagioclase, fassaite, spinel, diopside, and olivine. Accessory minerals include ilmenite (Fig. 11c), sulfides and Fe,Ni-metal. Plagioclase ranges in composition from oligoclase (An_{15}) to anorthite ($An_{90–100}$). Primary An-rich plagioclase is often intergrown with oligoclase; the latter appears to be a secondary phase in many cases formed during parent body metamorphism. One of these plagioclase-rich chondrules was described by Bischoff et al. (1994). The spinels are mostly euhedral and have a variable composition (see below). Fassaite in the chondrules typically occurs as thin bars within a feldspathic groundmass (Figs. 11b and 11d). In most cases olivine is zoned with the Fe content increasing towards the rim. The fayalite content of the olivine is sometimes as high as 48 mol%. Within two chondrules abundant Na-rich glass embedding olivine was found (Fig. 11a).

Al-Rich Fragments

Six Al-rich fragments are probably fragments of CAIs or chondrules. Almost all are spinel-rich except for one

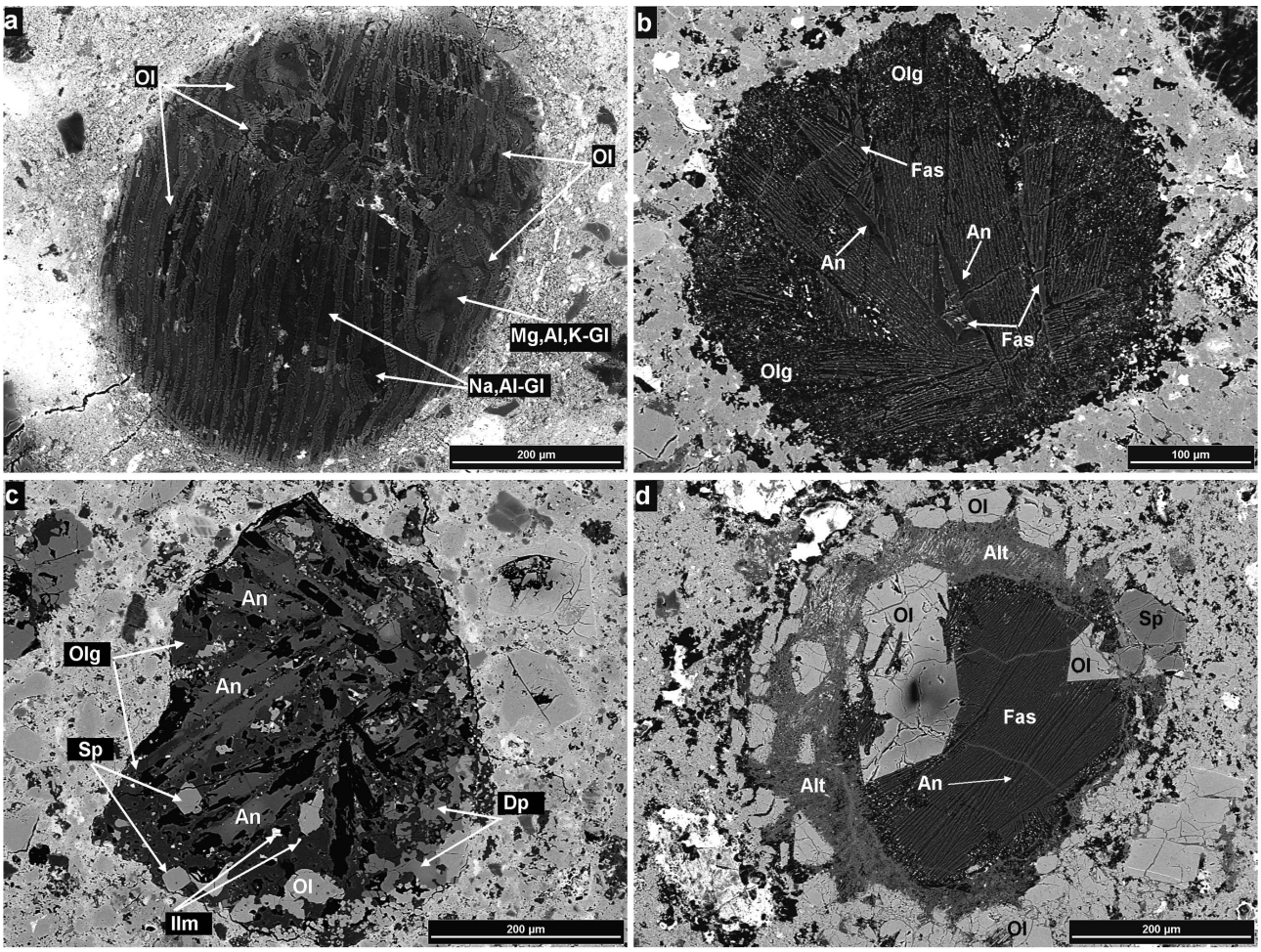


Fig. 11. BSE images of Al-rich chondrules. a) 753C/21 (NWA 753); forsteritic olivine bars (Ol) are enclosed within an Na,Al-bearing glass (Na,Al-Gl) and Mg, Al, K-bearing glass (Mg, Al, K-Gl). b) 755/13 (NWA 755); radiating fassaite (Fas) laths are surrounded by anorthitic plagioclase (An). Towards the rim oligoclase (Olg) is most probably replacing anorthite. c) D013B/183 (Dar al Gani 013); large fragment of a chondrule showing intergrowth of oligoclase (Olg) and anorthite (An), and euhedral spinel (Sp), olivine (Ol), diopside (Dp), and minor ilmenite (Ilm). d) DfrB/32 (Dhofar 1223); it looks like a compound chondrule with a porphyritic texture in the upper left and a radiating texture in the lower right. In the outer areas large (zoned) porphyritic grains of olivine (Ol), a large spinel (Sp), and some alteration products (Alt) occur. The chondrule interior has well-defined bars of fassaite (Fas) with anorthite (An) in their interstices.

hibonite-rich fragment. They clearly show broken edges (Fig. 12) and do not have any relationship with the matrix components.

Compositions of Minerals in CAIs from R Chondrites

Spinel

It is an abundant phase in almost all Al-rich inclusions and shows a wide range of composition (Table 2). Typically, spinel contains FeO. Spinels within inclusions from type 3 lithologies are often zoned and have less FeO, varying from <1–~20 wt% (Fig. 13). Typical spinel from metamorphosed R chondrite lithologies has ~20–25 wt% FeO, and also has high ZnO (up to 6.6 wt%: Table 2), frequently variable Cr_2O_3 (up to ~6 wt%; Table 2), and some NiO (up to ~0.5 wt%; Table 2). Some spinels from chondrule D013B/144 have high Cr_2O_3 (up to 18 wt%) and FeO (up to 35 wt%; Table 2).

Hibonite

This mineral is very rare in R-chondrite CAIs and quite variable in composition (Table 3). Except for hibonites from inclusion H030/L, which are very poor in TiO_2 and MgO, all others have considerable TiO_2 and MgO (Table 3). Due to their small grain size some analyses may be contaminated by surrounding phases (mainly spinel), leading to higher MgO and FeO concentrations (see Table 3). A plot of Ti versus Mg (per 19 oxygen atoms) shows that the points plot on the 1:1 line, consistent with a coupled substitution of $Mg^{+2} + Ti^{+4} \leftrightarrow 2Al^{+3}$ (Fig. 14a). A plot of Mg + Ti + Si + Fe versus Al + Cr showing the coupled substitution scheme indicates more clearly the different species involved in the coupled substitution process: $(Mg^{2+},Fe^{2+}) + (Si^{4+},Ti^{4+}) \leftrightarrow 2(Al^{3+},Cr^{3+})$ (Fig. 14b). Almost all the hibonites fall on the above mentioned substitution line. Under the optical microscope, hibonite shows blue, colorless and orange colors.

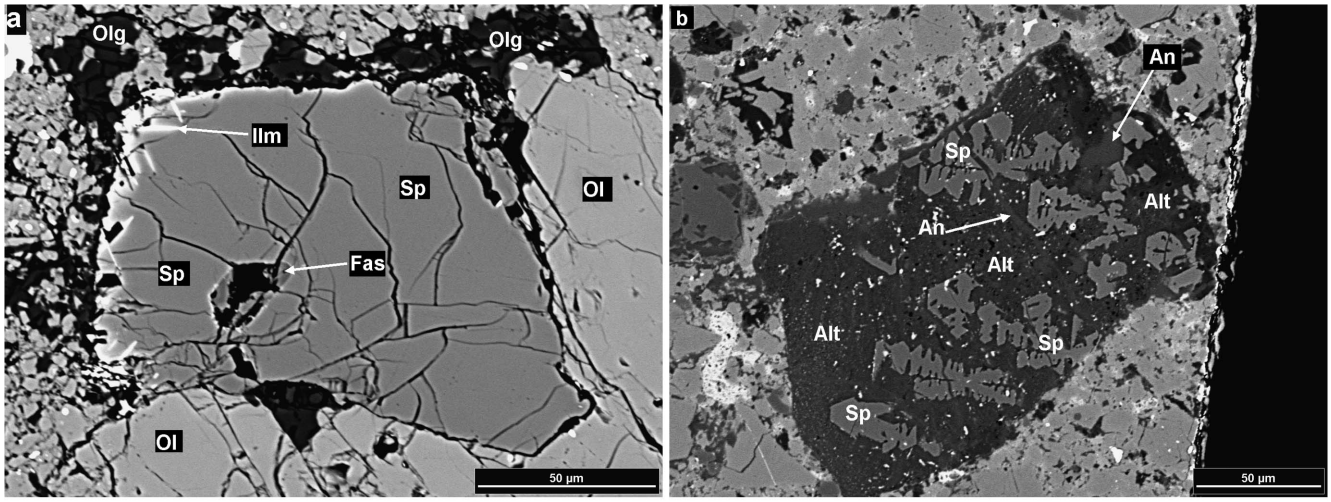


Fig. 12. BSE images of a) fragment 753_124/33 (NWA 753) is spinel-rich, with exsolution lamellae of ilmenite (Ilm) within the spinel (Sp); minor fassaite (Fas) is also present, and b) H030/2L (Hughes 030); spinel-rich fragment with minor anorthitic plagioclase (An) and abundant fine-grained alteration products (Alt). Spinels (Sp) have a skeletal texture suggestive of crystallization from a melt.

In the fassaite-rich spherule, 1476/124, it has a blue color, which may be due to the presence of Ti^{+3} (Ihinger and Stolper 1986). These two hibonites plot above the 1:1 substitution line for Mg and Ti atoms (Fig. 14a) and show an excess of Ti for the corresponding Mg atoms. This may indicate the presence of Ti^{+3} in these hibonite grains. Further, hibonites in the simple concentric spinel- and hibonite-rich inclusion H030/L show different appearances: (a) some grains are colorless because they have very low TiO_2 contents (Table 3) or they may have equilibrated under very oxidizing conditions (Ihinger and Stolper 1986); (b) some other grains of this inclusion show an orange color; and (c) additionally, some hibonites have small blue cores surrounded by thick colorless rims. Most probably our analysis reflects those of the colorless parts, because mineral analyses reveal that they have low TiO_2. Hibonite in fragment 2446B/5L is colorless to very light orange. Stoichiometric analysis indicates that Mg and Ti atoms have a perfect 1:1 correlation, which indicates absence of any Ti^{+3}, and the light orange tinge may be due to the Ti^{+4} (Ihinger and Stolper 1986). The other hibonite grains are too small for reliable optical analysis.

Fassaite and Diopside

Al-Ti-diopside, or subsilicic titanoan aluminian pyroxene (fassaite) (Morimoto et al. 1988) is one of the most abundant phases in CAIs from R chondrites. Al_2O_3 and TiO_2 vary from ~7 to ~30 wt% and ~1.5 to ~16 wt%, respectively (Table 4). MgO contents of fassaite decrease with increasing Al_2O_3 (Fig. 15b). Mg is in the M1 site in the fassaite crystal structure, and with increase in $CaAl_2SiO_6$ (CaTs-), Ti^{+3}-, and Ti^{+4}-bearing components the Mg is replaced by Ti^{+3}, Ti^{+4}, and Al. As a consequence, there is a simultaneous replacement of Si by Al in the tetrahedral site to maintain charge balance (Simon et al. 1991). This substitution is further depicted in the SiO_2 versus MgO, TiO_2 versus MgO, and TiO_2 versus Al_2O_3 plots (Fig. 15). Similar trends are seen in fassaite in coarse-grained inclusions in CV3 chondrites (Simon et al. 1991).

Diopside in CAIs mostly occurs as a rim layer. Its composition varies from Al-rich to pure diopside (Table 5). It also occurs in Al-rich chondrules. Al-diopside has Al_2O_3 contents varying from 1.5 to 18 wt% with little or no TiO_2.

Perovskite and Ilmenite

Perovskite is a rare phase in the R chondrite CAIs and is completely absent from Al-rich chondrules. It is present only in the least-altered CAIs of the most primitive type 3 fragments. In several cases perovskite cores are surrounded by ilmenite rims. Similar observations were made for perovskites in CAIs from ordinary chondrites (Bischoff and Keil 1983a, 1983c, 1984). The perovskites are very small, thus preventing reliable analyses in many cases, and the data in Table 6 include some contamination from the surrounding phases during EPM analysis.

In many Ca,Al-rich inclusions and in one Al-rich chondrule (D013B/183; Fig. 11), ilmenite occurs as an accessory phase. Due to the small grain size, quantitative analysis was difficult. Most ilmenites have about 2 wt% MgO, ~0.6 wt% MnO, and in some cases CaO (Table 6). All ilmenite probably formed by alteration of perovskite after the replacement of Ca by Fe during secondary alteration in the nebula or during thermal metamorphism on the meteorite parent body.

Plagioclase

Some of the CAIs and Al-rich chondrules have anorthite and labradorite which appear to be primary constituents of the Al-rich objects. Anorthites exist in the Ca,Al-rich inclusions, whereas all labradorites (except one in inclusion Afr/4L) are found in chondrules. The anorthite component in the

Table 2. Representative analyses of spinels from the Ca,Al-rich inclusions in R chondrites; all data in wt% and ordered according to the inclusions listed in Table 1; n.d.= not detected.

CAI no.	Incl.*	MnO	MgO	Al_2O_3	Cr_2O_3	SiO_2	CaO	FeO	TiO_2	NiO	ZnO	Total
RA/43A	1	0.18	15.9	67.0	0.41	<0.04	0.07	15.6	<0.01	<0.02	1.70	101.04
RA/43	1	0.16	10.1	63.2	0.10	0.12	<0.02	21.9	<0.05	0.34	1.90	98.00
RA/43	1	0.14	10.6	63.3	0.20	<0.04	<0.03	23.3	<0.03	0.38	1.92	100.08
RA/21	3	0.23	11.1	63.8	0.07	<0.03	<0.02	20.7	<0.03	0.24	3.4	99.73
RA/53	3	0.21	10.2	61.3	1.20	<0.03	0.05	22.8	<0.06	0.42	2.06	98.44
ShrB/41	1	0.13	11.3	60.7	2.70	<0.04	<0.03	21.1	0.14	0.14	1.32	97.64
D013B/118	1	n.d.	27.4	71.0	0.08	<0.01	<0.04	0.44	0.41	n.d.	<0.01	99.39
D013B/118	1	n.d.	27.4	70.9	n.d.	<0.03	0.05	1.01	0.40	n.d.	n.d.	99.90
D013B/118	1	<0.02	20.5	67.9	n.d.	0.45	0.07	7.9	0.30	n.d.	3.2	100.36
D013/44	1	n.d.	25.9	68.7	0.13	n.d.	0.06	2.18	<0.06	n.d.	n.d.	97.03
D013/44	1	<0.06	25.9	68.8	0.11	0.08	<0.04	2.32	0.24	<0.03	n.d.	97.59
D013B/15	1	<0.06	25.5	70.0	0.35	0.06	0.14	3.2	0.37	n.d.	n.d.	99.68
D013/23	1	<0.05	14.3	63.8	n.d.	0.06	0.09	17.7	0.17	n.d.	1.80	98.16
D013B/65	3	0.20	10.7	63.1	0.43	0.13	0.05	21.3	0.18	0.19	4.4	100.74
D013B/183	5	0.24	10.3	57.1	2.70	<0.02	<0.04	27.9	0.24	0.38	0.73	99.83
D013B/144	5	0.36	5.3	38.9	17.7	0.08	0.11	35.1	0.66	0.22	1.60	100.12
D417/43	3	0.22	10.9	58.6	2.21	<0.04	0.05	24.5	0.09	0.54	1.68	99.01
H030/22	3	0.10	9.9	60.5	1.05	0.36	0.64	21.0	1.37	0.13	4.1	99.20
H030/2L	6	0.09	11.8	62.8	1.33	<0.05	0.11	21.9	0.13	0.33	1.05	99.62
Dfr/53	3	0.14	18.6	67.5	n.d.	<0.03	0.06	12.8	0.34	<0.06	0.53	100.06
Dfr/53	3	0.09	18.7	66.8	n.d.	<0.02	0.08	13.2	0.26	0.11	0.62	99.91
Dfr/53	3	n.d.	16.5	65.6	n.d.	<0.04	<0.04	15.3	0.61	0.09	2.40	100.58
DfrB/2L	1	<0.01	11.6	62.8	0.22	0.07	0.18	19.0	<0.06	0.15	3.3	97.51
DfrB/32	5	0.08	10.8	60.9	0.49	0.14	0.08	20.6	0.10	0.30	3.5	97.14
753D/54	3	n.d.	20.6	65.1	0.93	0.06	0.08	10.0	0.68	<0.04	1.20	98.69
753D/54	3	<0.03	19.4	66.1	0.71	0.17	0.23	11.6	0.18	<0.01	0.55	99.01
753D/54	3	n.d.	15.7	63.0	1.23	<0.05	0.15	16.0	0.74	0.10	1.87	98.86
753D/54	3	n.d.	14.3	63.5	0.77	0.12	0.19	16.4	0.51	0.16	2.30	98.33
753B/62	1	0.14	19.0	65.9	n.d.	<0.02	0.07	10.7	0.22	<0.07	1.15	97.28
753/104	1	n.d.	19.8	67.6	n.d.	0.06	<0.02	11.5	0.15	0.09	0.37	99.59
753/104	1	<0.01	9.6	62.9	0.07	0.11	0.07	18.9	0.43	0.13	6.6	98.82
753/95	3	0.08	18.4	65.9	0.18	<0.03	<0.40	11.8	0.82	<0.03	0.46	98.18
753/12LB	6	<0.01	15.4	65.9	0.08	0.09	0.08	16.3	0.26	<0.02	0.91	99.05
753/11L	1	<0.04	13.9	65.7	0.33	0.12	<0.04	17.1	0.13	<0.06	2.09	99.58
753/35	3	0.13	11.5	63.2	0.70	<0.02	0.13	20.1	0.22	0.24	2.98	99.31
753_124/21	3	0.12	10.2	59.8	4.4	<0.05	<0.03	20.8	0.07	<0.04	2.90	98.62
753/22	3	0.09	11.1	61.6	1.45	0.24	n.d.	20.8	0.15	0.31	2.50	98.36
753/24	3	0.19	10.6	58.8	3.3	0.91	<0.02	20.9	<0.04	0.25	2.70	97.73
753/102	1	0.14	10.5	62.5	0.52	<0.05	<0.03	22.6	0.11	0.20	2.62	99.31
753/111	1	0.14	11.6	61.8	0.85	0.11	0.11	23.0	0.12	0.25	1.90	99.97
753_124/33	6	0.18	10.9	60.8	1.94	<0.03	<0.02	25.4	0.10	0.40	1.13	101.00
755/31	3	0.08	9.6	56.0	6.4	0.08	0.21	21.6	0.32	0.09	2.73	97.24
1471/23	3	0.21	11.3	64.0	0.08	0.07	<0.01	20.1	<0.01	0.30	3.3	99.52
1472/15	3	0.11	11.2	62.5	0.94	0.66	<0.02	20.4	0.23	0.41	2.30	98.92
1476C/8L	1	n.d.	27.4	70.3	n.d.	0.06	0.08	0.32	0.21	0.10	n.d.	98.47
1476C/8L	1	n.d.	27.1	70.2	<0.03	0.08	0.06	0.40	0.28	n.d.	n.d.	98.15
1476C/8L	1	n.d.	26.5	70.0	n.d.	0.08	0.07	0.90	0.28	n.d.	<0.05	97.88
1476C/8L	1	0.11	12.9	63.2	n.d.	0.14	0.37	19.0	0.09	<0.02	1.90	97.82
1476/83	1	<0.04	26.6	70.3	0.08	n.d.	<0.01	0.51	0.16	<0.07	n.d.	97.81
1476/83	1	n.d.	26.7	70.1	0.63	<0.03	<0.04	0.71	0.13	n.d.	n.d.	98.34
1476C/62B	3	n.d.	27.2	70.1	n.d.	0.21	0.39	0.82	0.24	<0.02	n.d.	98.99
1476C/62B	3	<0.02	25.1	68.3	0.29	0.70	0.54	2.78	0.41	n.d.	0.14	98.28
1476C/62B	3	n.d.	24.4	68.5	0.32	0.33	0.19	4.1	0.17	n.d.	n.d.	98.01
1476B/12	3	n.d.	20.6	66.1	n.d.	<0.04	0.11	9.7	0.23	n.d.	0.22	97.00
1476B/12	3	<0.02	15.8	64.6	n.d.	<0.04	0.08	15.3	0.27	n.d.	1.05	97.19
1566/32	1	0.12	11.6	64.6	0.45	<0.02	<0.01	20.6	0.16	0.13	1.89	99.66

Table 2. *Continued.* Representative analyses of spinels from the Ca,Al-rich inclusions in R chondrites; all data in wt% and ordered according to the inclusions listed in Table 1; n.d.= not detected.

CAI no.	Incl.*	MnO	MgO	Al_2O_3	Cr_2O_3	SiO_2	CaO	FeO	TiO_2	NiO	ZnO	Total
2446/84	1	<0.05	17.7	65.8	n.d.	0.28	0.15	13.9	0.21	<0.07	1.17	99.33
2446/112	1	0.12	14.4	65.1	0.49	<0.01	0.06	16.9	0.31	0.14	1.83	99.40
2446/33	1	0.13	10.2	62.3	0.33	0.84	0.67	20.8	<0.03	0.20	3.4	98.90
2446/12	3	<0.06	10.5	63.7	n.d.	<0.02	0.09	21.6	0.18	<0.07	3.8	100.15
2446/23	1	0.12	10.3	61.7	0.14	0.34	0.18	24.3	0.49	0.15	2.98	100.72

Incl.* = Inclusion number indicates the inclusion type: (1) simple concentric spinel-rich inclusion, (3) complex spinel-rich CAI, (5) Al-rich chondrule, and (6) Al-rich (spinel-rich) fragment.

Table 3. Representative analyses of hibonite from the Ca,Al-rich inclusions in R chondrites; all data in wt%; n.d.= not detected.

CAI no.	Incl.*	MnO	MgO	Al_2O_3	Cr_2O_3	SiO_2	CaO	FeO	TiO_2	Total
RA/911	1	<0.01	2.21	85.5	n.d.	0.25	7.9	1.28	3.5	100.65
RA/911	1	n.d.	2.08	85.2	0.27	0.33	8.0	1.03	3.4	100.31
H030/L	1	<0.01	n.d.	91.7	n.d.	<0.01	8.7	0.61	0.13	101.16
H030/L	1	<0.05	<0.01	92.5	0.08	0.05	8.3	0.36	0.16	101.52
H030/L	1	n.d.	<0.01	92.6	n.d.	0.04	8.4	0.30	0.15	101.50
H030/L	1	n.d.	<0.01	92.6	0.32	0.05	8.5	0.42	0.15	102.05
1476/124	2	<0.02	0.96	87.6	0.19	n.d.	8.8	0.34	2.47	100.38
1476/124	2	n.d.	1.07	88.0	0.16	n.d.	8.7	0.19	2.50	100.62
2446/12	3	<0.01	1.35	87.6	n.d.	0.16	7.5	0.57	2.49	99.69
2446/122	3	n.d.	2.44	84.1	n.d.	0.36	8.3	1.00	4.3	100.51
2446B/5L	6	<0.02	1.18	88.1	0.13	0.14	8.6	0.68	2.29	101.14
2446B/5L	6	n.d.	1.34	87.8	n.d.	0.06	8.5	0.58	2.60	100.88
2446B/8L	1	n.d.	2.26	84.1	<0.02	0.35	8.3	0.86	4.1	99.99
2446/12	3	n.d.	3.1	82.3	n.d.	0.14	7.9	0.86	5.7	100.00

Incl.* = Inclusion number indicates the inclusion type: (1) simple concentric spinel-rich CAI, (2) fassaite-rich spherule, (3) complex spinel-rich CAI, and (6) Al-rich (spinel-rich) fragment.

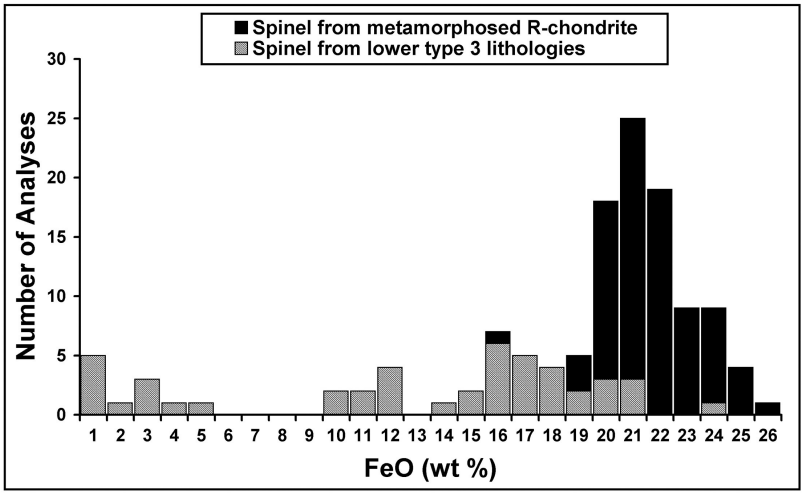


Fig.13. Histogram showing the FeO contents (in wt%) of representative spinel grains. A maximum of four spinel analyses from each Al-rich object, but only one analysis from individual grains is included in the histogram. Spinels from type 3 lithologies are indicated by dashed gray (compare Table 2); one spinel in a chondrule has up to 35 wt% FeO.

labradorite ranges from $An_{56–67}$. Almost all the CAIs from the type 4 or higher petrologic types are enriched in oligoclase (~$An_{8–20}$). This oligoclase most probably formed from fine-grained, Na,Al-(Cl)-rich secondary alteration products found in type 3 lithologies due to metamorphism and recrystallization. Some inclusions also have minor abundances of andesine ($An_{30–45}$) (Table 7). All oligoclase has a minor component of orthoclase ($Or_{2–5}$).

Na,Al-(Cl)-Rich Alteration Products, Nepheline, and Sodalite

Many of the CAIs are heavily altered and have significant amounts of Na,Al-rich alteration products, which

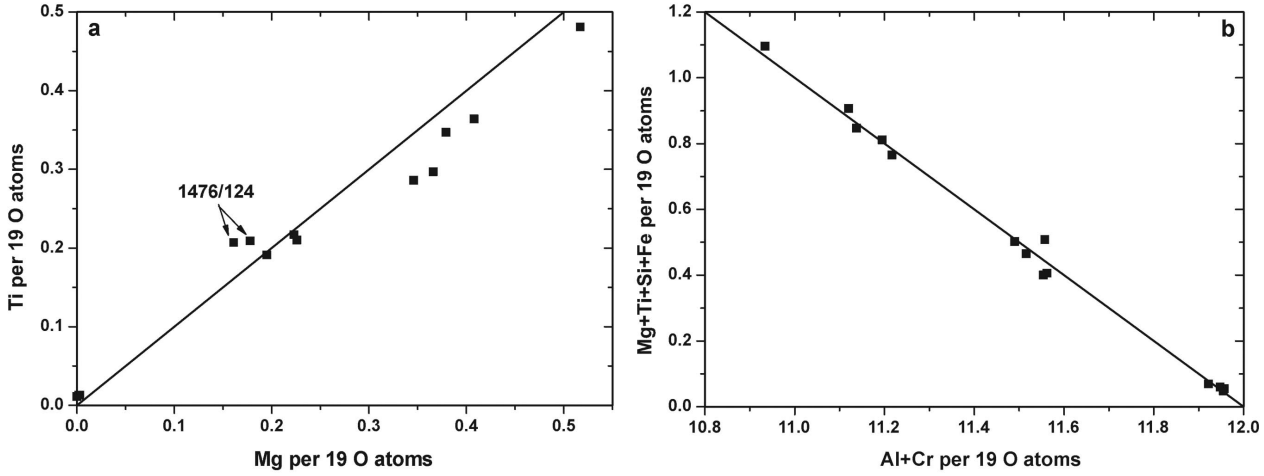


Fig. 14. a) Plot of Mg and Ti cations in a stoichiometric hibonite crystal with 19 oxygen atoms consistent with the coupled substitution of Mg and Ti for Al. b) Mg + Ti + Si + Fe versus Al + Cr plot for the same stoichiometric hibonite grains with the substitution line.

are most probably nepheline, sodalite, or a mixture of both. Quantitative mineral analysis is difficult because of porosity (resulting in low totals), small grain size, and fine-grained intergrowths. Many of the studied alteration-rich areas also contain relicts of primary minerals. Thus, many analyses are contaminated by intergrown and/or surrounding phases. Several analyses are certainly close to stoichiometric nepheline and sodalite (Table 8). In the higher petrologic types, nepheline and sodalite were replaced by oligoclase (see above). Considering all analyses, these alteration products are rich and variable in the volatile elements Na, K, and Cl (Na_2O: 4–23 wt%, K_2O: up to 6.2 wt%, Cl: up to 7.3 wt%), and Al_2O_3 is always high (~25–40 wt%).

Olivine

Olivine occurs mostly in Al-rich chondrules, plus in a few CAIs. Most of the olivines that appear to be located inside CAIs, are actually in matrix-filling indentations. But some olivine is native to the CAIs, for example the olivines found within the fassaite-rich spherule shown in Fig. 5b. In addition, native olivine occurs in some rims (Fig. 3d). It is highly fayalitic and similar in composition to matrix olivine of R chondrites, whereas the olivines from the spherule have variable compositions (Fig. 5b). No forsteritic olivine has been found within the CAIs.

On the other hand, compositions of olivine from chondrules vary from pure forsterite to highly fayalitic. In some cases it is zoned from forsteritic cores to fayalitic rims. Fig. 16, a histogram of olivine compositions, shows a peak at Fa ~37–38 mol%, which is similar to the normal fayalite content of olivine in equilibrated R chondrites. Some olivine has Fa contents as high as 48 mol%, similar in composition to those in the matrix of primitive type 3 lithologies from R chondrites (Bischoff 2000).

DISCUSSION

Size and Abundance of Ca,Al-Rich Inclusions in Rumuruti Chondrites and other Chondrite Groups

Various chondrite groups differ not only in bulk and mineral chemistry and in grain size, but also in the relative abundance of components like chondrules, CAIs and matrix, and in the sizes of components like chondrules and Ca,Al-rich inclusions. Based on MacPherson et al. (1988) and MacPherson (2003) the maximum sizes of individual CAIs in various components can be summarized: (1) the cm-sized CAIs in CV3 chondrites are about one order of magnitude larger than the largest CAIs in other chondrite groups (~1 mm). (2) The largest Ca,Al-rich inclusion found in CM chondrites has a size of 1.7 mm (MacPherson and Davis 1994), but most are less than 0.5 mm. (3) Considering the CO3 chondrites all of the inclusions studied by Russell et al. (1998a, 2000a) are smaller than ~1 mm in size and most are even smaller than 0.5 mm. (4) CAIs in CR chondrites are similar in size to the CO3 inclusions. The largest are also on the order of 1 mm (Aléon et al. 2002; MacPherson 2003), but most are smaller than 300 μm (Weber and Bischoff 1997). (5) The largest CAI within the CH chondrite Acfer 182 has a size of 450 μm, but most are much smaller (<300 μm; Weber et al. 1995). Ca,Al-rich inclusions from the CH chondrite ALH85085 are even smaller (largest: 110 μm; Grossman et al. 1988). (6) The largest known CAI in ordinary chondrites is 480 μm, but most are significantly smaller (Bischoff and Keil 1983c, 1984; MacPherson 2003). (7) The inclusions from the enstatite chondrites are the smallest among the chondrite groups ranging from 50–140 μm (Bischoff et al. 1985; Fagan et al. 2000).

As stated above, the size of the inclusions in R chondrite

Table 4. Representative analyses of fassaite from Ca,Al-rich inclusions in R chondrites; all data in wt%; n.d. = not detected.

CAI no.	Incl.[a]	Na_2O	MnO	MgO	Al_2O_3	Cr_2O_3	SiO_2	CaO	FeO	TiO_2	Total
RA/53	3	0.09	0.07	14.6	15.1	0.27	45.2	21.3	2.40	1.80	100.82
RA/53	3	0.19	0.07	14.7	7.9	n.d.	50.0	23.7	1.06	1.16	98.78
D013B/15	1	n.d.	n.d.	10.8	19.2	n.d.	36.9	24.3	0.68	8.9	100.78
D013B/118	1	0.08	<0.03	8.1	20.5	0.19	35.7	24.0	1.43	9.1	99.14
D013/24	3	<0.01	n.d.	6.5	23.1	0.35	32.5	24.3	0.62	11.1	98.49
D013/44	1	<0.02	n.d.	7.5	27.1	0.30	29.7	24.8	0.92	8.3	98.63
H030/22	3	<0.02	0.06	13.8	8.3	0.55	48.0	25.6	0.54	3.8	100.67
H030/22	3	0.09	n.d.	11.4	12.9	0.19	43.1	24.9	1.17	5.1	98.89
H030/22	3	0.04	0.08	12.2	12.3	0.24	44.0	24.8	0.74	4.6	99.00
Dfr/53	3	n.d.	<0.04	5.4	25.2	n.d.	29.7	24.6	0.13	14.7	99.77
Dfr/53	3	n.d.	n.d.	5.9	23.2	n.d.	30.5	24.7	0.47	14.7	99.47
Dfr/53	3	n.d.	n.d.	5.3	24.1	0.52	29.6	24.2	0.26	15.6	99.58
Dfr/53	3	<0.02	n.d.	5.7	23.6	0.19	30.9	24.8	0.25	14.5	99.96
Dfr/53	3	<0.02	<0.04	6.6	24.1	n.d.	32.1	24.5	0.34	12.3	100.00
Dfr/53	3	0.06	n.d.	5.9	24.8	0.19	29.6	24.0	0.67	14.7	99.92
Dfr/23	2	n.d.	n.d.	11.5	17.4	0.55	43.5	25.2	0.40	1.21	99.76
Dfr/75	3	0.34	<0.03	7.3	21.3	0.19	33.4	23.5	1.13	11.7	98.89
DfrB/12	5	0.04	0.08	15.6	7.5	0.56	49.6	23.0	0.23	2.94	99.55
DfrB/12	5	<0.02	n.d.	14.7	8.2	0.29	49.0	23.0	0.31	3.9	99.42
753/35	3	0.03	n.d.	14.8	11.2	0.05	45.9	22.4	0.36	4.5	99.24
753/52	3	0.03	<0.04	5.2	25.0	0.13	31.2	24.5	0.79	13.0	99.89
753/52	3	n.d.	0.07	5.1	24.8	n.d.	32.4	23.2	1.34	11.9	98.81
753/131	3	0.26	n.d.	7.0	23.9	n.d.	34.6	23.7	1.08	7.6	98.13
753/131	3	0.09	<0.02	10.5	17.6	n.d.	42.6	24.5	0.48	3.7	99.49
753/ 42	3	0.16	<0.02	9.5	15.8	0.06	39.8	23.6	3.60	6.1	98.64
753B/14	2	n.d.	0.09	17.8	13.0	n.d.	46.4	18.9	0.34	1.54	98.07
753B/33	3	0.30	<0.05	8.4	20.6	0.10	35.8	23.5	0.94	6.9	96.59
753B/33	3	<0.02	n.d.	10.9	17.0	0.35	40.2	23.4	1.14	5.1	98.19
753D/64	3	<0.02	n.d.	6.1	23.0	<0.02	31.2	24.6	1.00	13.7	99.64
753/31	3	0.10	n.d.	13.2	12.7	0.74	46.4	24.5	0.47	2.69	100.80
753/12LA	3	0.11	n.d.	12.9	11.5	n.d.	46.1	24.8	1.56	2.99	99.96
753D/74	3	0.07	0.08	12.1	14.3	0.32	44.3	25.1	1.09	3.4	100.77
753_124/33	6	<0.02	n.d.	7.8	22.2	0.38	35.8	25.2	1.11	7.2	99.68
755/13	6	0.23	<0.02	16.3	13.4	0.75	46.0	19.5	1.25	2.48	99.93
755/33	5	n.d.	n.d.	11.5	16.5	0.19	43.4	25.4	0.17	2.26	99.42
755/33	5	<0.01	<0.05	11.4	16.9	0.11	42.8	24.8	0.31	2.96	99.34
1472/1711	3	0.73	<0.01	7.0	21.4	0.19	34.8	23.8	1.08	10.2	99.21
1476/124	2	n.d.	<0.01	5.7	29.6	0.16	34.4	25.5	0.27	4.0	99.64
1476/124	2	<0.01	0.06	6.9	27.0	0.16	37.5	25.2	0.35	2.70	99.88
1476C/62A	1	0.11	<0.02	6.8	21.9	0.40	33.6	23.6	0.72	13.1	100.25
1476C/8L	1	0.04	<0.01	4.9	24.6	n.d.	31.4	25.0	0.36	12.6	98.92
1476C/8L	1	n.d.	<0.02	3.8	27.1	0.16	28.2	24.3	0.16	16.1	99.84
1476C/8L	1	n.d.	n.d.	3.2	28.1	0.29	26.0	23.9	0.17	16.9	98.56
1478/35	3	<0.02	n.d.	7.5	26.9	0.19	38.8	25.3	0.12	1.34	100.17
1478/35	3	n.d.	<0.04	7.0	28.0	<0.02	37.5	24.6	0.15	1.92	99.29
2446/71B	5	0.03	<0.02	17.2	7.5	0.22	49.8	22.2	0.27	2.30	99.54
2446/71B	5	n.d.	n.d.	17.3	7.7	1.21	49.4	21.6	0.22	2.74	100.17
2446/71A	3	n.d.	<0.01	6.1	25.7	n.d.	30.3	23.8	1.20	13.1	100.27
2446/ 23	1	0.08	<0.02	14.6	7.3	n.d.	49.8	24.1	1.19	1.55	98.64
2446/33	1	0.08	0.08	9.5	19.3	0.17	38.5	22.8	1.85	6.6	98.88
2446/33	1	0.05	<0.01	9.6	19.7	0.27	38.7	22.8	1.91	6.8	99.84
2446B/1L	3	<0.01	<0.02	5.2	26.4	0.10	28.6	22.8	2.12	13.7	98.95

Incl.[a] = Inclusion number indicates the inclusion type: (1) simple concentric spinel-rich inclusion, (2) fassaite-rich spherule, (3) complex spinel-rich CAI, (5) Al-rich chondrule, and (6) Al-rich (spinel-rich) fragment.

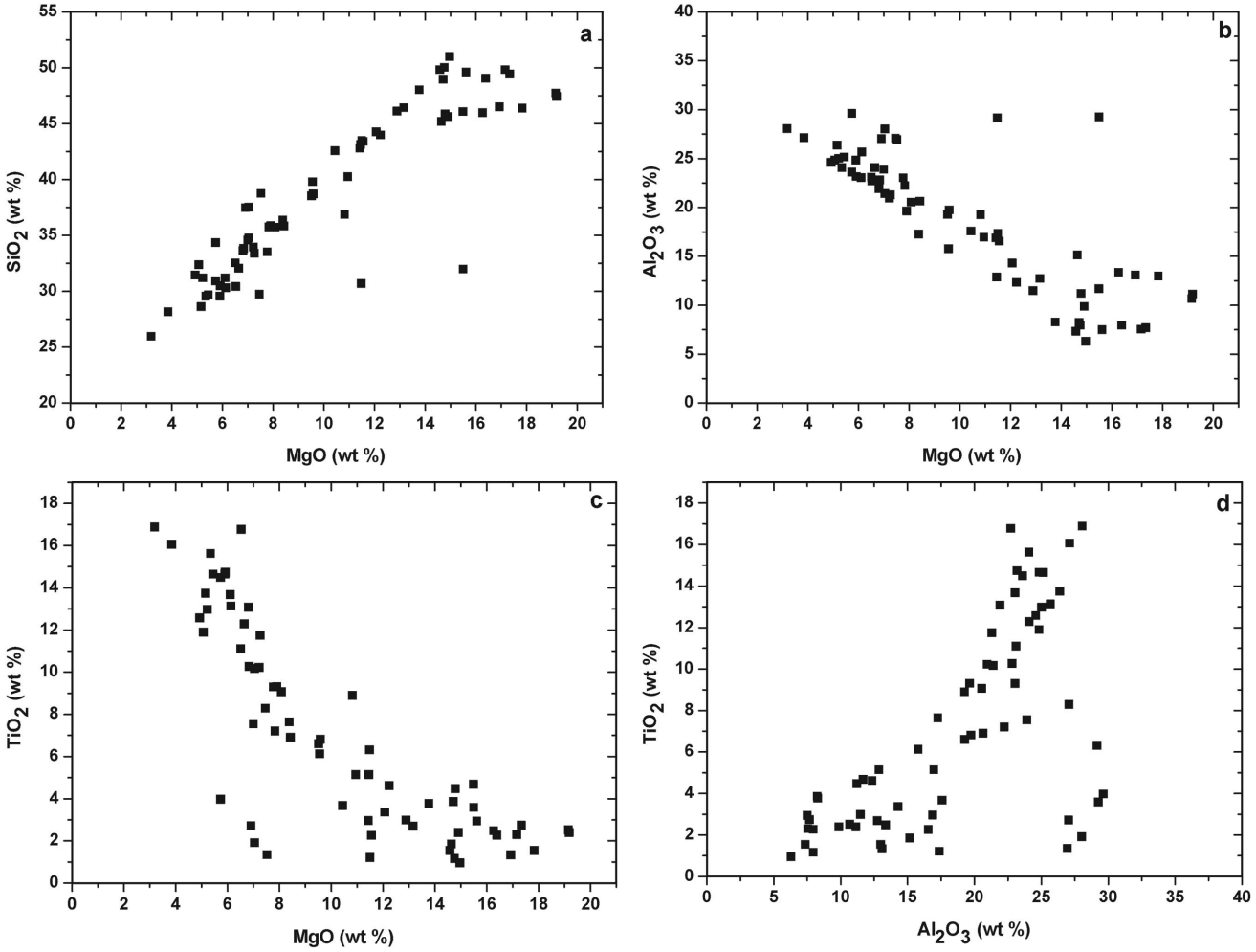


Fig. 15. a) SiO_2 versus MgO for fassaites shows a positive correlation, due to the fact that Si and Mg are in tetrahedral and M1 sites, respectively. With decrease in Mg, there is a corresponding increase in CaTs component along with Al substitution for Si in the tetrahedral site. b) Al_2O_3 versus MgO further shows the CaTs versus Di substitution in the fassaite crystal. c) TiO_2 versus MgO, with all Ti calculated as Ti^{+4}, depicts the substitution of Mg by Ti^{+3}, Ti^{+4} in the M1 site along with the Ca-Ts substitution. d) TiO_2 versus Al_2O_3 shows the combined effect of Ti^{+3}, Ti^{+4}, and Al in the M1 site and corresponding substitution of Al for Si to maintain charge balance.

are very small. The largest CAI is 600 μm in size (Fig. 8b), whereas most are <200 μm in apparent size similar to the CAIs in CH, ordinary, and enstatite chondrites. According to the size of CAIs in different chondrite groups, the following sequence can be given: CV > CM ≈ CO > CR > RC ≥ CH > OC > EC.

In order to determine the abundances of CAIs in various lithologies of R chondrites, the surface area of thin sections, of distinct R chondrite fragments, and of the existing Ca,Al-rich inclusions were measured. In some R chondrites not a single CAI was found (Table 1). We cannot rule out that Ca,Al-rich inclusions could be found in larger additional thin sections of the same meteorite. However, the abundance of CAIs will certainly be close to 0%. The highest abundances of refractory inclusions were found within two highly unequilibrated, type 3 clasts within the R chondrites NWA 753 and NWA 2446 with 0.08 and 0.07 vol%, respectively. The abundance of CAIs is clearly higher than that in ordinary and enstatite chondrites (Bischoff and Keil 1984; Bischoff et al. 1984, 1985; Guan et al. 2000a,b; Fagan et al. 2000, 2001; Kimura et al. 2002). We agree with the trend for the CAI abundance given by Russell (1998): CC > RC > OC > EC.

Mineralogical Differences between CAIs in Different Lithologic Types

The dominant phases in CAIs of type 3 lithologies in R chondrites are spinel (with variable compositions), fassaite, nepheline + sodalite (or mixtures of both, often considered here as fine-grained Na,Al-rich alteration products), and diopside in the rim. Accessory hibonite, anorthite, olivine, ilmenite, and perovskite, ± troilite occur. On the other hand, Ca,Al-rich inclusions in R chondrites or fragments of R-chondrite breccias which have seen significant thermal annealing during metamorphism (e.g., ~>R3.8 ± 0.1 – R6) have different mineralogical constituents. Here, Fe-rich spinel (20–26 wt%

Table 5. Representative analyses of diopside from Ca,Al-rich inclusions in R chondrites; all data in wt%; n.d. = not detected.

CAI no.	Incl.[a]	Na_2O	MnO	MgO	Al_2O_3	Cr_2O_3	SiO_2	CaO	FeO	TiO_2	Total
RA/43A	1	0.04	0.09	17.5	4.6	0.16	52.6	24.8	0.64	0.15	100.58
D013B/15	1	n.d.	<0.02	17.5	1.95	0.27	53.6	25.6	1.22	0.37	100.53
D013B/118	1	0.25	0.10	14.3	3.6	n.d.	51.8	23.7	5.8	0.83	100.38
D013B/183	5	0.54	0.18	14.8	0.62	0.17	53.7	23.2	6.0	0.02	99.20
D013/24	3	0.03	n.d.	15.6	5.5	n.d.	50.7	25.0	1.24	0.66	98.73
D013/44	1	0.03	<0.01	15.2	8.3	0.16	50.0	25.3	1.24	0.21	100.46
D013B/65	3	<0.02	<0.04	18.0	2.75	n.d.	53.4	24.1	1.32	0.77	100.40
D417/43	3	0.25	0.05	15.9	0.47	n.d.	54.3	23.1	5.1	<0.01	99.18
Dfr/75	3	0.15	0.09	16.0	3.8	0.13	51.0	23.9	2.84	0.29	98.20
753/46	3	n.d.	n.d.	17.2	3.4	0.11	53.4	25.2	0.62	0.25	100.18
753/52	3	<0.02	<0.03	18.0	3.6	n.d.	54.6	24.0	1.02	0.09	101.36
753/6L	3	n.d.	0.09	16.5	4.4	0.44	53.0	24.4	1.00	0.26	100.09
753/104B	1	0.05	0.15	16.0	6.9	0.38	52.2	24.6	1.01	0.16	101.45
753/111	1	0.13	0.07	16.2	4.6	n.d.	51.5	24.3	1.02	1.22	99.05
753/131	3	n.d.	n.d.	16.3	5.1	0.08	51.2	24.6	0.17	1.02	98.47
753/154	1	n.d.	n.d.	16.0	6.1	0.45	51.4	24.0	1.04	0.38	99.37
753/52	3	0.07	0.07	15.8	6.6	0.16	50.9	25.1	0.88	1.34	100.92
753/12LA	3	0.34	n.d.	14.9	3.7	<0.02	52.8	23.8	4.7	0.56	100.82
753/143	1	0.05	n.d.	15.8	6.0	0.08	51.2	23.6	1.36	1.00	99.10
753B/13	1	0.22	0.07	15.0	3.3	0.16	51.6	23.3	4.3	0.21	98.16
753B/33	3	<0.02	<0.02	17.0	3.4	n.d.	53.3	25.0	0.88	n.d.	99.62
753B/62	1	<0.01	n.d.	13.5	13.5	0.05	46.6	23.8	1.18	0.45	99.09
753B/62	1	0.07	n.d.	16.9	2.96	0.46	53.2	24.5	0.99	0.22	99.30
753C/31	3	0.05	0.06	14.7	7.3	0.13	49.9	24.7	0.71	0.48	98.03
753D/54	3	0.06	n.d.	17.1	1.87	n.d.	53.9	25.5	0.80	0.16	99.39
753D/54	3	n.d.	n.d.	16.0	5.9	0.27	50.7	25.8	0.57	0.97	100.21
753D/64	3	0.03	<0.03	18.4	0.52	0.38	54.6	25.2	1.07	n.d.	100.23
753D/74	3	0.09	0.08	17.9	1.58	n.d.	53.5	25.5	1.39	<0.01	100.05
753D/54	3	<0.02	n.d.	16.4	4.8	n.d.	50.7	25.4	0.31	1.71	99.34
753_124/23	1	0.10	<0.01	15.1	6.9	n.d.	49.8	25.0	0.57	1.21	98.69
753_124/23	1	0.09	n.d.	17.7	1.95	0.38	53.4	24.5	1.17	0.34	99.53
753_124/12L	1	0.05	n.d.	16.1	5.9	n.d.	50.4	24.6	1.04	0.21	98.30
1472/12	1	0.09	n.d.	18.0	1.28	n.d.	54.7	25.3	0.89	0.44	100.71
1472/56	1	n.d.	<0.04	17.8	2.63	n.d.	53.8	24.8	0.80	0.72	100.59
1472/1711	3	n.d.	n.d.	18.1	0.48	n.d.	55.2	25.1	1.02	<0.04	99.95
1472/1711	3	0.09	<0.01	17.9	1.07	0.58	55.3	25.0	0.54	0.08	100.57
1476/22	5	n.d.	0.15	18.6	4.5	0.22	52.7	21.3	0.60	2.40	100.48
1476/83	1	<0.02	n.d.	18.2	1.60	n.d.	54.6	24.2	0.41	0.34	99.37
1476/83	1	n.d.	n.d.	17.7	3.5	n.d.	52.6	25.0	0.40	1.09	100.29
1476/124	2	<0.01	n.d.	11.7	16.3	n.d.	45.4	25.7	0.55	<0.04	99.70
1476/22	5	n.d.	<0.04	19.1	4.3	0.18	52.2	20.8	0.82	1.90	99.34
1476B/12	3	n.d.	n.d.	15.5	6.8	n.d.	51.3	25.7	0.69	0.42	100.41
1476C/54	3	n.d.	<0.03	15.5	6.3	0.19	51.8	25.5	0.33	0.24	99.89
1476C/62A	1	0.07	<0.04	17.7	4.2	0.13	52.4	24.1	0.77	0.29	99.70
1476C/62B	3	0.03	0.09	13.0	15.3	0.10	45.5	24.8	0.45	1.00	100.28
1476C/ 62B	3	0.05	0.05	15.0	9.1	n.d.	49.8	24.6	0.43	0.67	99.71
2446/33	1	n.d.	<0.01	17.2	3.2	0.30	53.0	23.4	0.71	0.05	97.87
2446/71B	5	0.05	n.d.	17.2	3.7	0.32	54.1	22.2	0.36	0.07	98.03
2446/71B	5	n.d.	n.d.	17.5	2.96	<0.05	53.3	24.0	0.70	0.34	98.85
2446/71B	5	<0.01	n.d.	18.0	2.11	0.19	54.0	25.2	0.50	<0.01	100.02
2446/84	1	n.d.	n.d.	18.8	0.89	n.d.	54.4	24.1	1.01	0.19	99.42
2446/84	1	0.10	n.d.	17.7	2.10	0.19	53.5	25.2	0.89	0.16	99.84
2446/63	4	n.d.	n.d.	17.4	0.68	0.13	53.5	24.5	1.96	<0.02	98.19
2446/112	1	0.05	<0.04	17.1	3.1	0.31	52.9	25.0	0.69	0.80	100.00
2446/122A	3	<0.02	<0.02	16.7	4.9	0.13	52.2	23.5	2.12	0.14	99.73
2446B/1L	3	n.d.	<0.03	17.8	3.2	0.22	53.2	24.6	0.87	1.02	100.95
2446B/54	3	0.05	n.d.	17.7	2.62	0.24	53.6	23.8	0.82	0.56	99.39

Incl.[a] = Inclusion number indicates the inclusion type: (1) simple concentric spinel-rich inclusion, (2) fassaite-rich spherule, (3) complex spinel-rich CAI, (4) complex diopside-rich inclusion, and (5) Al-rich chondrule.

Table 6. Analyses of perovskite and ilmenite from the Ca,Al-rich inclusions in R chondrites; all data in wt%; n.d.= not detected.

CAI no.	Incl.[a]	MnO	MgO	Al_2O_3	Cr_2O_3	SiO_2	CaO	FeO	TiO_2	Total
Perovskite										
D013B/118	1	<0.02	n.d.	0.62	n.d.	0.14	40.3	0.54	55.9	97.53
D013B/118	1	n.d.	0.03	0.56	n.d.	0.16	40.3	0.45	56.6	98.20
D013B/118	1	n.d.	0.12	0.41	0.24	0.09	39.0	0.76	57.2	97.83
D013B/118	1	n.d.	<0.01	0.68	n.d.	0.17	40.7	0.44	56.7	98.70
Dfr/53	3	<0.04	<0.02	0.21	0.21	0.08	40.7	0.31	57.8	99.37
Ilmenite										
753_124/12L	1	0.66	2.67	0.03	0.12	0.03	0.17	42.7	52.3	98.73
753_124/12L	1	0.65	2.52	0.13	n.d.	0.20	0.15	43.2	52.1	99.02
753_124/12L	1	0.67	2.68	0.04	0.51	0.02	0.14	43.6	53.0	100.73
1472/119	3	0.62	1.99	0.22	0.24	0.11	0.10	42.2	51.5	96.98

Incl.[a] = Inclusion number indicates the inclusion type: (1) simple concentric spinel-rich inclusion and (3) complex spinel-rich CAI.

FeO) and oligoclase (~$An_{8–20}$) occur as major phases; additional minor phases include anorthite, fassaite, olivine, ilmenite, and diopside. Almost all CAIs in metamorphosed lithologies have similar mineralogical assemblages. Oligoclase was never found in CAIs from lower type 3 R chondrites and has to be of post-accretionary, metamorphic origin. Spinels in Ca,Al-rich inclusions from lower type 3 lithologies have lower hercynite components than spinels in metamorphosed lithologies (Fig. 13) and are commonly zoned. In some inclusions FeO is <1 wt%. These spinels also have low ZnO. Thus, secondary processes during metamorphism (see below) have led to replacement of Mg by Fe and Zn. In addition, perovskite is only found in CAIs in lithologies of lower petrologic type. In more highly metamorphosed rocks, only ilmenite is observed. CaO in perovskite is replaced by FeO to form ilmenite during secondary alteration. In several cases, grains have cores of perovskite and rims of ilmenite. Similar observations were made for the perovskite/ilmenite assemblage in CAIs from ordinary chondrites (Bischoff and Keil 1983a, 1983c, 1984). These secondary processes will be discussed below.

Similar CAIs within other Groups of Chondrites

CAIs in the R chondrites are distinct. Although there are significant similarities with CAIs in other chondrite groups, there are also definite differences which show that the CAI assemblages within the R-chondrites are unique. The CAIs from R chondrite are, considering the sizes of the inclusions, as stated already above, very small, similar to the CAIs in ordinary and enstatite chondrites. Corundum (Bar-Matthews et al. 1982; MacPherson et al. 1983, 1984), melilite, grossite (Weber and Bischoff 1994, 1997; Weber et al. 1995), and $CaAl_2O_4$ (Ivanova et al. 2002) are completely absent, and hibonite is a very rare phase. Due to these and other mineralogical characteristics, we conclude that CAIs similar to melilite-rich or -bearing Type A and B CAIs mainly found in CV3 chondrites (like Allende; e.g., Grossman et al. 1975; MacPherson and Grossman 1979; Grossman 1980; MacPherson et al. 1988; Brearley and Jones 1998, and references therein) are not present in R chondrites. Grossite-bearing inclusions, which are common in CH chondrites (Weber and Bischoff 1994; Weber et al. 1995) and rare in CO, CM, and CR chondrites (MacPherson 2003; Simon et al. 1994; Fagan et al. 2000) are completely absent in R chondrites. Amoeboid olivine aggregates known from many other chondrite groups (MacPherson et al. 1988; MacPherson 2003, and references therein) were also not observed in R chondrites.

However, many of the inclusions studied here are similar to CAIs in other chondrite groups (e.g., carbonaceous and ordinary chondrites). In CV chondrites, some types of inclusions occur that are in some respects similar to inclusions in R chondrites. These inclusions are the fine-grained, spinel-rich inclusions with abundant secondary alteration products (e.g., Cohen et al. 1983; Kornacki et al. 1983; Kornacki and Wood 1984; Brearley and Jones 1998, and references therein). Both the simple concentric spinel-rich inclusions and the complex spinel-rich inclusions in the R chondrites are quite similar to the concentric objects and chaotic objects in the Mokoia CV3 chondrite (Cohen et al. 1983), although the latter have high-Al phyllosilicates (HAP) which are completely absent in the R-chondrite CAIs.

In general, however, there are much stronger similarities to Ca,Al-rich inclusions in the metamorphosed subtypes of CO3 chondrites (types 3.5–3.7; e.g., Russell et al. 1998a), and in particular in the new Moss CO3 chondrite that has been recently studied (Bischoff and Schmale 2007). Strong similarities between CAIs in Moss and R chondrites certainly exist for the simple concentric spinel-rich CAIs. Similar objects with cores of spinel, perovskite, and pyroxene which are mantled by feldspathoids and diopside (Davis 1985; Davis and Hinton 1986; Frost and Symes 1970) have also been described from Ornans and Lancé. Simple concentric spinel-rich CAIs in R chondrites are also similar to the "nodular" spinel-pyroxene inclusions from CM chondrites (MacPherson and Davis 1994), some spinel nodules in CR chondrites (Aléon et al. 2002), and spinel-pyroxene inclusions in the CO3 chondrites (Russell et al. 1998a). The latter inclusions in the

Table 7. Representative analyses of plagioclase from the Ca,Al-rich objects in R chondrites; all data in wt%; n.d.= not detected; An = anorthite content in mol%.

CAI no.	Incl.[a]	Na_2O	K_2O	MnO	MgO	Al_2O_3	Cr_2O_3	SiO_2	CaO	FeO	TiO_2	Total	An (mol%)
RA/21	3	9.1	0.32	n.d.	n.d.	23.2	<0.03	64.1	4.4	0.48	n.d.	101.63	20.7
RA/53	3	10.2	<0.03	<0.02	0.04	23.4	n.d.	65.3	2.48	0.37	<0.02	101.86	11.8
RB/81	5	10.2	0.98	n.d.	<0.02	20.4	0.08	67.1	1.67	0.70	n.d.	101.15	7.8
ShrB/41	1	10.2	0.52	n.d.	0.25	20.5	n.d.	65.4	2.16	1.04	n.d.	100.07	10.1
Afr/4L	3	7.8	0.24	n.d.	<0.03	25.6	n.d.	58.6	6.5	0.51	n.d.	99.23	31.2
Afr/61	5	10.0	0.69	n.d.	n.d.	22.6	n.d.	65.4	1.77	0.22	n.d.	100.68	8.6
Afr/111	5	10.4	0.39	n.d.	<0.02	23.0	n.d.	64.6	1.97	0.15	n.d.	100.53	9.2
Afr/111	5	6.1	0.11	<0.02	<0.01	27.9	0.43	55.0	8.4	0.30	n.d.	98.27	43.1
D013B/183	5	0.28	n.d.	n.d.	<0.03	36.1	n.d.	43.5	19.7	0.25	0.07	99.94	97.7
D013B/183	5	0.06	n.d.	<0.01	n.d.	36.7	n.d.	43.3	20.4	0.07	0.15	100.70	99.3
D013B/88	5	9.4	0.09	n.d.	<0.01	23.5	n.d.	62.9	4.3	0.58	n.d.	100.78	20.2
D013B/119	3	10.0	0.15	n.d.	<0.01	21.8	0.19	65.3	2.24	0.59	n.d.	100.32	10.9
D013B/144	5	6.7	0.04	<0.03	n.d.	26.8	<0.03	56.9	8.3	0.50	n.d.	99.30	40.6
D013B/183	5	10.1	0.10	<0.03	0.07	21.6	0.08	64.8	3.00	0.17	n.d.	99.95	14.0
DfrB/32	5	2.16	0.06	n.d.	0.63	31.5	n.d.	47.1	16.0	0.90	0.08	98.44	80.0
753/35	3	n.d.	n.d.	n.d.	<0.02	36.1	n.d.	43.4	20.1	0.18	0.22	100.02	100.0
753/61	5	1.13	0.08	n.d.	0.19	33.8	0.22	46.1	17.3	1.09	<0.02	99.94	89.2
753/6L	3	0.18	<0.01	n.d.	n.d.	35.8	0.35	43.8	19.5	0.43	n.d.	100.07	98.3
753/6L	3	0.08	<0.01	<0.03	0.13	35.7	n.d.	43.2	19.2	0.85	<0.05	99.27	99.3
753/12LA	3	0.05	n.d.	n.d.	0.04	36.2	0.50	42.9	19.7	0.65	n.d.	100.04	99.7
753/1L	3	10.0	0.66	<0.01	0.11	21.9	n.d.	65.4	2.35	0.32	n.d.	100.75	11.1
753/35	3	10.1	0.53	n.d.	<0.03	22.1	<0.05	65.9	2.40	0.29	<0.05	101.47	11.3
753/24	3	9.8	0.46	n.d.	0.04	21.1	n.d.	65.5	2.55	0.48	<0.01	99.94	12.3
753B/22	5	2.45	0.07	n.d.	<0.01	31.2	0.16	47.7	15.1	0.44	<0.03	97.17	77.1
753B/6L	3	9.4	0.41	n.d.	<0.01	21.0	<0.05	64.2	2.77	0.45	0.07	98.36	13.6
753C/51	3	0.03	<0.01	<0.03	<0.02	36.0	n.d.	43.0	19.7	0.58	<0.04	99.42	99.7
753C/51	3	0.11	<0.03	0.06	<0.01	35.3	n.d.	43.2	19.5	0.64	n.d.	98.85	99.0
753_124/21	3	9.6	0.70	n.d.	0.07	20.7	0.25	66.4	2.11	0.41	<0.01	100.25	10.4
755/13B	5	1.20	0.07	<0.01	0.04	34.1	n.d.	45.6	18.0	0.23	0.15	99.41	89.1
755/13B	5	1.12	0.05	n.d.	<0.01	34.3	n.d.	45.2	18.2	0.25	0.19	99.33	89.8
755/13B	5	9.9	0.52	n.d.	0.08	20.7	0.08	64.6	2.61	0.35	n.d.	98.84	12.3
755/13B	5	9.5	0.34	n.d.	<0.01	21.4	n.d.	65.0	2.80	0.53	n.d.	99.58	13.7
755/31	3	9.6	0.62	n.d.	<0.01	21.5	n.d.	64.4	2.80	0.31	<0.01	99.25	13.6
755/33	5	10.1	0.63	<0.01	n.d.	21.4	<0.05	64.6	2.57	0.18	n.d.	99.54	11.9
1471/23	3	10.6	0.89	n.d.	<0.02	21.0	0.41	66.2	2.03	0.55	n.d.	101.70	9.1
1471/3L	3	9.8	0.56	n.d.	0.04	21.4	n.d.	64.8	2.52	0.54	<0.04	99.70	12.0
1472/1711	3	0.05	n.d.	n.d.	0.03	35.6	n.d.	43.4	20.0	0.39	<0.04	99.51	99.7
1472/1711	3	<0.02	n.d.	n.d.	0.05	37.1	0.28	43.5	20.2	0.35	<0.04	101.55	99.7
1472/1711	3	0.04	0.04	<0.03	0.06	36.4	n.d.	43.7	20.1	0.43	0.08	100.89	99.3
1472/15	3	9.9	0.50	n.d.	<0.03	21.8	n.d.	65.4	2.48	0.38	<0.06	100.55	11.8
1472/15	3	10.1	0.54	n.d.	<0.02	21.5	n.d.	65.7	2.57	0.52	<0.03	100.98	11.9
1472/117	3	10.2	0.50	<0.02	0.04	22.4	n.d.	65.3	2.60	0.39	n.d.	101.45	12.1
1472/119	3	10.3	0.55	<0.02	0.04	22.2	n.d.	65.8	2.70	0.73	<0.02	102.36	12.3
1476/22	5	1.30	0.24	n.d.	0.04	35.1	n.d.	42.8	18.3	0.33	<0.03	98.15	87.4
1476/22	5	0.48	n.d.	n.d.	0.09	34.9	0.19	43.2	19.0	0.49	<0.05	98.43	95.7
1476C/101	3	9.9	0.69	<0.02	0.06	20.7	0.16	64.7	2.30	0.40	n.d.	98.93	10.9
1478/35	3	9.6	0.74	0.06	<0.02	22.3	0.19	65.3	2.35	0.10	n.d.	100.66	11.4
1478/35	3	9.5	0.47	<0.02	<0.02	22.1	n.d.	64.7	2.44	0.40	<0.04	99.69	12.1
1478/12	1	9.9	0.45	n.d.	0.05	20.9	n.d.	64.2	2.50	0.68	<0.03	98.71	12.1
2446/71B	5	1.64	<0.01	n.d.	0.41	33.8	0.37	46.9	15.7	0.42	0.07	99.32	84.1

Incl.[a] = Inclusion number indicates the inclusion type: (1) simple concentric spinel-rich inclusion, (3) complex spinel-rich CAI, and (5) Al-rich chondrule.

CO3 chondrites (Russell et al. 1998a) consist of aggregates of spinel nodules with accessory perovskite and sometimes hibonites, and are rimmed by aluminous diopside.

The simple concentric spinel- and hibonite-rich CAIs are mineralogically similar to the hibonite-hercynite inclusions in CO3 chondrites (Russell et al. 1998a), to single concentric

Table 8. Analyses of fine-grained alteration products dominated by sodalite and nepheline from the Ca,Al-rich inclusions in R chondrites; all data in wt%; n.d.= not detected.

CAI no.	Incl[a]	Na_2O	K_2O	MgO	Al_2O_3	Cl	Cr_2O_3	SiO_2	CaO	FeO	SO_3	TiO_2	NiO	Total
Sodalite														
RA/43A	1	14.3	0.19	0.59	35.2	6.7	n.d.	42.7	1.26	0.67	0.14	<0.03	<0.04	101.82
RA/43A	1	12.8	0.12	0.68	36.9	6.8	<0.02	39.1	0.82	1.53	0.18	<0.04	n.d.	98.99
RA/43B	1	20.5	n.d.	0.27	32.9	7.3	0.08	36.3	n.d.	1.08	n.d.	0.19	n.d.	98.62
RA/53	3	23.0	<0.01	0.05	34.3	7.1	<0.05	37.2	<0.02	0.32	<0.01	<0.03	<0.03	102.13
ShrB/41	1	16.8	<0.02	0.39	32.5	7.3	0.30	39.8	n.d.	1.20	0.72	<0.01	0.22	99.27
ShrB/41	1	17.3	0.03	0.98	34.3	6.3	0.43	37.0	<0.02	2.06	0.80	<0.05	0.33	99.61
753/104B	1	18.3	0.08	0.10	35.4	6.9	n.d.	39.9	0.25	0.95	n.d.	0.22	<0.06	102.16
753C/31	3	18.8	0.04	0.61	29.8	6.0	n.d.	41.0	1.14	0.91	0.10	0.10	0.32	98.83
1472/56	1	12.2	0.05	0.70	38.1	6.9	<0.05	39.6	0.55	0.62	0.38	<0.05	0.38	99.59
Nepheline														
RA/21	3	15.0	6.1	0.16	36.1	<0.05	0.22	42.1	2.05	0.49	n.d.	<0.05	n.d.	102.32
DfrB/2L	1	14.7	4.7	0.07	33.5	<0.03	0.29	44.4	2.28	0.23	<0.06	<0.02	<0.06	100.35
DfrB/2L	1	12.6	4.4	0.20	32.6	0.15	n.d.	45.3	2.75	0.24	0.27	<0.02	0.72	99.26
753B/34	1	16.4	3.2	0.24	32.2	n.d.	n.d.	44.4	1.44	1.36	<0.05	0.22	0.07	99.58
753B/34	1	17.4	3.3	n.d.	33.5	<0.01	n.d.	42.7	1.09	0.55	<0.02	<0.05	0.09	98.71
753B/34	1	15.3	3.3	0.31	33.3	<0.01	n.d.	43.8	1.03	1.17	0.14	0.18	0.90	99.45

Incl.[a] = Inclusion type indicates the inclusion type: (1) simple concentric spinel-rich inclusion and (3) complex spinel-rich CAI.

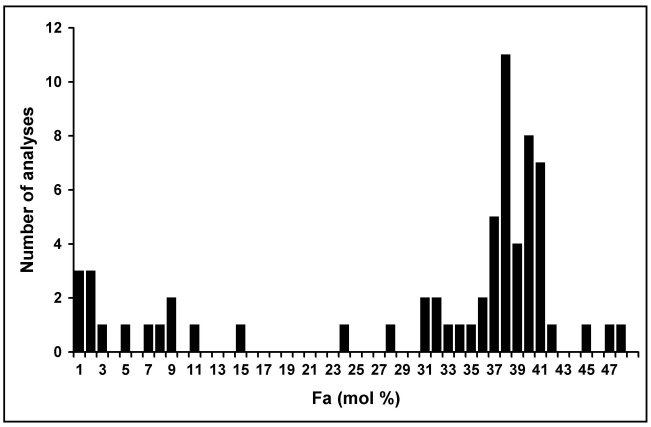


Fig. 16. Fayalite content of olivine in CAIs and Al-rich chondrules.

objects in the Moss CO3 chondrite (Bischoff and Schmale 2007), and to the spinel-hibonite inclusions, SHIBs, in CM chondrites (Ireland 1988). Simple concentric spinel-rich CAIs that also have abundant Na,Al-(Cl)-rich alteration products have been also described from several CO3 chondrites (e.g., Tomeoka et al. 1992; Russell et al. 1998a; Bischoff and Schmale 2007).

The complex spinel-rich inclusions also bear resemblance to the irregular spinel-rich aggregates with accessory perovskite and hibonite, rimmed by aluminous diopside, found in Isna, Ornans, and Lancé (Frost and Symes 1970; Methot et al. 1975; Davis 1985; Davis and Hinton 1986). Mineralogically, the complex spinel- and hibonite-rich CAIs (Fig. 6) bear resemblance to the hibonite-hercynite inclusions in the CO3 chondrites (Russell et al. 1998a) and some spinel-hibonite inclusions in CM chondrites (Ireland 1988). The complex spinel- and fassaite-rich inclusions (Fig. 8) are similar to the Ca-pyroxene-nepheline-rich inclusions in the Moss CO3 chondrite (Bischoff and Schmale 2007). The complex spinel- and Na,Al-alteration product-rich inclusions (Fig. 9) resemble best the altered spinel-pyroxene inclusions in CO3 chondrites (Russell et al. 1998a), complex, fine-grained, Ca-pyroxene-nepheline-rich inclusions in the Moss CO3 chondrite (Bischoff and Schmale 2007), and complex spinel-nepheline-rich inclusions within the Yamato-791717 CO3 chondrite (Tomeoka et al. 1992).

Considering the three fassaite-rich spherules (Fig. 5), the hibonite-bearing object resembles inclusions reported earlier from other chondrite groups (hibonite-bearing microspherules; e.g., Kurat 1975; Ireland et al. 1991; Tomeoka et al. 1992; Simon et al. 1998; Grossman et al. 1988; Kimura et al. 1993; Russell et al. 1998a). After their first discovery within the Lancé CO3 chondrite by Kurat (1975) similar objects were reported to occur in CH, CM and CO3 chondrites. Ireland et al. (1991) studied one inclusion from the Lancé CO3 chondrite (found by Kurat (1975)) and two from the Murchison CM chondrite. Two of these inclusions have hibonite laths within a glassy groundmass. The other spherule from Murchison has a core of rounded hibonite grains with perovskites, and a rim of Fe-silicate material. Russell et al. (1998a) also found two such glassy spherules in CO3 chondrites. Simon et al. (1998) and Tomeoka et al. (1992) described one spherule each from Murray (CM2) and Yamato 791717 (CO3), respectively. These two inclusions have pyroxene enclosing the hibonite laths. All the spherules range in size from ~50 to ~170 μm. Considering the mineral assemblage the spherules in the R chondrite are distinct: one spherule has abundant spinel and pyroxene and the other euhedral grains of spinel and olivine laths embedded in pyroxene (Fig. 5b).

Although many mineralogical similarities may point to a genetic link between CAIs in R and CO3 chondrites, some similarities with CAIs from ordinary and enstatite chondrites occur. (1) CAIs from the ordinary and enstatite chondrites are very small (<50 μm). (2) As in the R chondrites, the spinel-pyroxene inclusions constitute a significant population of CAIs in the ordinary and enstatite chondrites (Bischoff and Keil 1983c, 1984; Bischoff et al. 1984, 1985; Guan et al. 2000a,b; Fagan et al. 2001; Kimura et al. 2002).

Secondary Alteration—Nebular or Parent Body, or Both

The overwhelming number of Ca,Al-rich inclusions have remarkably high abundances of phases rich in the volatile elements Na, K, Cl, Fe, and Zn. Only a very small portion of the studied CAIs in Rumuruti chondrites show minor secondary alteration. Where and when did this alteration occur?

In most cases, Ca,Al-rich inclusions in R chondrites are fine-grained and spinel-rich. Many authors have described fine-grained, spinel-rich CAIs in carbonaceous and ordinary chondrites. Grossman and Ganapathy (1975, 1976) and Grossman et al. (1975) describe Allende fine-grained feldspathoid-, grossular-, spinel-, and pyroxene-bearing inclusions with high volatile element abundances. Grossman and Ganapathy (1976) proposed that these inclusions may have formed by simultaneous condensation of volatiles and refractory lithophile elements. Similar inclusions from carbonaceous chondrites with high abundances of volatile element-bearing phases were described by e.g., Wark and Lovering (1977), Wark (1979), Tomeoka et al. (1992), Russell et al. (1998a), and Bischoff and Schmale (2007).

The setting for the formation of the secondary phases is a controversial topic and there are two different opinions: (a) low-temperature reactions in the solar nebula prior to their accretion into the parent body are suggested by several authors (e.g., Wark 1981; Hashimoto and Grossman 1985; McGuire and Hashimoto 1989; Davis et al. 1994); (b) low-grade metamorphism in the asteroidal bodies is advocated by others (e.g., Krot et al. 1995). Recent studies of short-lived radionuclides such as ^{26}Al and ^{36}Cl present within the secondary phases show that multiple alteration events have affected the CAIs from different chondrite groups (e.g., Lin et al. 2005; Fagan et al. 2007; Ushikubo et al. 2007).

Fagan et al. (2007) found resolvable ^{26}Mg excesses in the secondary minerals (grossular, feldspar, nepheline) within the Allende CAIs. On the other hand they found secondary minerals within the same inclusions having no ^{26}Mg. Grossular and secondary feldspars in one CAI have excesses of ^{26}Mg consistent with an initial ^{26}Al/^{27}Al ~4.5×10^{-5}, indicating a nebular setting for their formation. Secondary minerals with much smaller or no ^{26}Mg excesses must have formed much (>3 Myr) later. Based on these results Fagan et al. (2007) suggest that "the timing of secondary alteration is consistent with, but does not necessarily require, alteration in an asteroidal setting."

Similarly, studies of ^{36}Cl-, and ^{26}Al isotopes of secondary minerals in a moderately altered type B2 inclusion from the Allende CV3 chondrite by Ushikubo et al. (2007) show excess of ^{36}S in the sodalites and no resolvable ^{26}Mg excess in anorthite and sodalites implying multiple episodes of secondary alteration that happened as early as within the first 1.5 Myr of CAI formation and lasted as late as 5.7 Myr.

Nebular Alteration

In earlier studies, Bischoff and Keil (1983a, 1984) suggested that Ca,Al-rich inclusions in ordinary chondrites probably formed by agglomeration of refractory dust and low-temperature, Fe-, Na-, and K-rich materials, and that secondary diffusion and reactions between the low- and high-temperature components led to their present mineral assemblages and textures. Bischoff and Keil (1984) found that irregularly-shaped inclusions in ordinary chondrites have undergone even more extensive alteration than most CAIs in carbonaceous chondrites. Various authors suggested that most of the secondary alteration in Ca,Al-rich inclusions was pre-accretionary and occurred in the solar gas (e.g., Wark and Lovering 1977; Grossman 1980; MacPherson et al. 1981; Wark 1981; Bischoff and Keil 1984). The high degree of secondary alteration may indicate that there was easy access of the nebular gas to the primary phases at lower temperatures. Allen et al. (1978), MacPherson et al. (1981), and Wark (1981) discussed the scenario that the fine-grained secondary assemblage of nepheline, grossular, anorthite, and wollastonite in many CAIs from carbonaceous chondrites could have formed by decomposition mainly of melilite as a result of reactions with the nebular gas. Many CAIs from type 3 lithologies in R chondrites studied here have high abundances of Na,Al-(Cl)-rich fine-grained alteration products. These products occur in the form of nepheline and/or sodalite or as mixtures of both. In this case we also suggest that they formed by nebular alteration due to the replacement of mainly melilite by nepheline/sodalite-bearing secondary intergrowths.

Asteroidal Alteration

The inclusions found in the metamorphosed lithologies of R chondrites have high abundances of oligoclase (Fig. 6). The fine-grained secondary alteration products in the form of nepheline and/or sodalite or as mixtures of both are gone. This oligoclase has a similar composition as the oligoclase occurring in the matrix and within relict chondrules of equilibrated lithologies. As already suggested above, the nepheline/sodalite phases are replaced by oligoclase. Thus, oligoclase is certainly a post-accretionary product and formed by parent body processes. We suggest that the formation of oligoclase is certainly caused by parent body metamorphism.

Secondary Alteration—Nebular and Asteroidal

The replacement of CaO by FeO in perovskite has often been observed in Ca,Al-rich inclusions from various

chondrite groups (e.g., Cohen et al. 1983; Bischoff and Keil 1984; Hashimoto and Grossman 1985; Kornacki and Wood 1985; McGuire and Hashimoto 1989; Tomeoka et al. 1992). Some of the perovskites are completely replaced by ilmenite, whereas others have still a perovskite core rimmed by ilmenite. Typically, within the neighboring spinel MgO is replaced by FeO + ZnO. The situation is less clear, whether all the chemical replacements within the spinel and the perovskite/ilmenite assemblages occurred by processes in the nebula or by thermal alteration (metamorphism) on the R chondrite parent body. Considering similar replacements in CAIs from ordinary chondrites Bischoff and Keil (1984) suggested that the original mineral assemblage altered in the nebula: "Mainly volatile rich materials entered the refractory objects as a gas, reacted with the constituents and produced secondary phases." In the case of the replacement processes within spinels and perovskites we suggest that the chemical exchange processes started in the nebula. We also suggest that these chemical alterations by diffusion continued during parent body metamorphism. In analogy, Fe-rich spinel is a typical mineral in Ca,Al-rich inclusions from the metamorphosed CK chondrites as a result of metamorphic equilibration (e.g., MacPherson and Delaney 1985; Noguchi 1993; Geiger and Bischoff 1995).

In summary, most inclusions found in R chondrites were affected by several different alteration processes, including early alteration in the nebula and late modifications on the R chondrite parent body.

THE MOST PRIMITIVE Ca,Al-RICH INCLUSIONS IN R CHONDRITES.

Basically all inclusions in R chondrites are affected by some kind of secondary alteration processes. However, in some inclusions these effects are very small. All CAIs with only minor alteration products were found in lower type 3 lithologies (Bischoff 2000). Some criteria for considering an inclusion to be representative of primary origin are: a) the presence of Mg-spinels instead of spinels having high concentrations of FeO and ZnO; b) the presence of perovskite instead of ilmenite, c) the absence of any Na,Al-rich alteration products, d) the absence of any post accretion metamorphic products (such as oligoclase), e) the presence of pure anorthite, if plagioclase is present at all.

No inclusion does fulfill all these criteria. However, based on these criteria, we have classified some of the inclusions as quite primitive. These are: a) Inclusion 1476/83 from NWA 1476 (Fig. 1b), a simple concentric inclusion having an almost Fe-free spinel core and a rim of diopside and minor fassaite below the rim. b) CAIs D013/44 (Fig. 3a) and D013B/118 (Fig. 3b) from DaG 013; these inclusions are simple concentric spinel- and fassaite-rich inclusions having Mg-spinel cores abundant fassaite and perovskites (the latter only in D013B/118; Fig. 3b). The diopsides rimming both inclusions are Fe-poor. Although these inclusions are grouped under the most primitive and primary inclusions, they still have a low abundance of Na-rich alteration products and/or some Fe at the spinel edges (Fig. 3).

The fassaite-rich spherules shown in Fig. 5 appear to be of primary origin, solidified from melt droplets. Inclusion 1476/124 from NWA 1476 (Fig. 5a) has hibonite laths, and the other two have spinel as the second most abundant phase after fassaite. The object Dfr/23 from Dhofar 1223 shown in Fig. 5b is not poor in FeO and has skeletal laths of olivine with varying Fa-contents. Based on the texture of the grains both olivines appear to have formed in situ. Since the backscattered electron image and elemental mapping do not show zoning of spinels and olivines, significant secondary element equilibration between the spherule and the matrix, or between the two olivines (which are chemically different) within the object can be ruled out. We do not have any clear explanation, why two relatively unzoned olivines coexist within this spherule. We suggest that it formed by melting of a heterogeneous (Fe-containing) precursor and crystallization of euhedral spinels and skeletal olivine. The object probably contained some FeO at the time of its formation, but severe parent body alteration leading to olivine equilibration during metamorphism can be ruled out.

CONCLUSION

Ca,Al-rich inclusions in Rumuruti chondrites are slightly more abundant than in ordinary chondrites and less common than in carbonaceous chondrites. Our observations confirm the trend given by Russell (1998): The abundance of CAIs in various chondrite groups decreases from CC > RC > OC > EC. CAIs in Rumuruti chondrites have abundant fine-grained Na,Al-(Cl)-rich alteration products. These inclusions were certainly altered during solar nebula and parent body processes. Especially Ca,Al-rich inclusions from metamorphosed R chondrites or metamorphosed lithologies in R chondrite breccias have been severely modified. Besides "primary" nebular alteration strong indications for planetary alteration are detectable in the form of the replacement of nepheline/sodalite by oligoclase. Replacement of perovskite by ilmenite and the incorporation of FeO and ZnO in the spinels exchanging MgO are probably the result of nebular and planetary alteration.

Acknowledgments–We thank Jasper Berndt-Gerdes (Münster) for assistance in the microprobe work and Ulla Heitmann and Thorsten Grund for technical support. We also thank Sara Russell, Steve Simon, and Tim Fagan of constructive reviews and the associate editor Christine Floss for thoughtful comments. We also appreciate the help of Klaus Keil (Hawai'i) in editing the manuscript and the loan of two Rumuruti thin sections from the Museum für Naturkunde in Berlin. This study is part of the dissertation of S. S. Rout at the Institut für Planetologie (Westfälische Wilhelms-Universität Münster).

Editorial Handling—Dr. Christine Floss

REFERENCES

Aléon J., Krot A. N., and McKeegan K. D. 2002. Calcium-aluminum-rich inclusions and amoeboid olivine aggregates from the CR carbonaceous chondrites. *Meteoritics & Planetary Science* 37:1729–1755.

Allen J. M., Grossman L., Davis A. M., and Hutcheon I. D. 1978. Mineralogy, textures and mode of formation of a hibonite-bearing Allende inclusion. Proceedings, 9th Lunar and Planetary Science Conference. pp. 1209–1233.

Armstrong J. T. 1991. Quantitative elemental analysis of individual microparticles with electron beam instruments. In *Electron probe quantitation*, edited by Heinrich K. F. J. and Newbury D. E. New York: Plenum Press. pp. 261–315.

Bar-Matthews M., Hutcheon I. D., MacPherson G. J., and Grossman L. 1982. A corundum-rich inclusion in the Murchison carbonaceous chondrite. *Geochimica et Cosmochimica Acta* 46: 31–41.

Berlin J. 2003. Mineralogisch-petrographische Untersuchungen an der chondritischen Breccie Rumuruti. Diploma Thesis, Institut für Mineralogie, Museum für Naturkunde, Berlin, Germany.

Binns R. A. and Pooley G. D. 1979. Carlisle Lakes (a): A unique oxidized chondrite (abstract). *Meteoritics* 14:349–350.

Bischoff A. 2000. Mineralogical characterization of primitive, type 3 lithologies in Rumuruti chondrites. *Meteoritics & Planetary Science* 35:699–706.

Bischoff A. and Keil K. 1983a. Ca,Al-rich chondrules and inclusions in ordinary chondrites. *Nature* 303:588–592.

Bischoff A. and Keil K. 1983b. Ca,Al-rich chondrules and inclusions in ordinary chondrites: Evidence for a related genesis of ordinary and carbonaceous chondrites (abstract). 14th Lunar and Planetary Science Conference. pp. 47–48.

Bischoff A. and Keil K. 1983c. Catalog of Al-rich chondrules, inclusions and fragments in ordinary chondrites. Special Publication No. 22, University of New Mexico, Institute of Meteoritics, Albuquerque NM, USA. pp. 1–33.

Bischoff A. and Keil K. 1984. Al-rich objects in ordinary chondrites: Related origin of carbonaceous and ordinary chondrites and their constituents. *Geochimica et Cosmochimica Acta* 48:693–709.

Bischoff A. and Schmale K. 2007: Ca,Al-rich inclusions within the Moss CO3 chondrite–indications for severe secondary alteration (abstract #1561). 38th Lunar and Planetary Science Conference. CD-ROM.

Bischoff A. and Schultz L. 2004. Abundance and meaning of regolith breccias among meteorites (abstract). *Meteoritics & Planetary Science* 39:A15.

Bischoff A. and Srinivasan G. 2003. ^{26}Mg-excess in hibonites of the Rumuruti chondrite Hughes 030. *Meteoritics & Planetary Science* 38:5–12.

Bischoff A., Keil K., and Stöffler D. 1984. Perovskite-hibonite-spinel-bearing, refractory inclusions and Ca,Al-rich chondrules in enstatite chondrites. *Meteoritics* 19:193–194.

Bischoff A., Keil K., and Stöffler D. 1985. Perovskite-hibonite-spinel-bearing inclusions and Al-rich chondrules and fragments in enstatite chondrites. *Chemie der Erde* 44:97–106.

Bischoff A., Palme H., and Spettel B. 1989. Al-rich chondrules from Ybbsitz H4 chondrite—Evidence for formation by collision and splashing. *Earth and Planetary Science Letters* 93:170–180.

Bischoff A., Palme H., Ash R. D., Clayton R. N., Schultz L., Herpers U., Stöffler D., Grady M. M., Pillinger C. T., Spettel B., Weber H., Grund T., Endreß M., and Weber D. 1993a. Paired Renazzo-type (CR) carbonaceous chondrites from the Sahara. *Geochimica et Cosmochimica Acta* 57:1587–1603.

Bischoff A., Palme H., Schultz L., Weber D., Weber H. W., and Spettel B. 1993b. Acfer 182 and paired samples, an iron-rich carbonaceous chondrite: Similarities with ALH 85085 and relationship to CR chondrites. *Geochimica et Cosmochimica Acta* 57:2631–2648.

Bischoff A., Geiger T., Palme H., Spettel B., Schultz L., Scherer P., Loeken T., Bland P., Clayton R. N., Mayeda T. K., Herpers U., Meltzow B., Michel R., and Dittrich-Hannen B. 1994. Acfer 217-A new member of the Rumuruti chondrite group (R). *Meteoritics* 29:264–274.

Bischoff A., Weber D., Bartoschewitz R., Clayton R. N., Mayeda T. K., Spettel B., and Weber H. W 1998. Characterization of the Rumuruti chondrite regolith breccia Hughes 030 (R3-6) and implications for the occurrence of unequilibrated lithologies on the R-chondrite parent body (abstract). *Meteoritics & Planetary Science* 33:A15–A16.

Bischoff A., Scott E. R. D., Metzler K., and Goodrich C. A. 2006. Nature and origins of meteoritic breccias. In *Meteorites and the early solar system II*, edited by Lauretta D. S. and McSween H. Y. Jr. Tucson: The University of Arizona Press. pp. 679–712.

Brearley A. J., and Jones R. H. 1998. Chondritic meteorites. In *Planetary materials*, edited by Papike J. J. Reviews in Mineralogy, vol. 36. Washington, D. C.: Mineralogical Society of America. pp. 3-01–3-398.

Cohen R. E., Kornacki A. S., and Wood J. A. 1983. Mineralogy and petrology of chondrules and inclusions in the Mokoia CV3 chondrite. *Geochimica et Cosmochimica Acta* 47:1739–1757.

Connolly H. C. Jr., Zipfel J., Grossman J. N., Folco L., Smith C., Jones R. H., Righter K., Zolensky M., Russell S. S., Benedix G. K., Yamaguchi A., and Cohen B. A. 2006. The Meteoritical Bulletin, No. 90. *Meteoritics & Planetary Science* 41:A1383–A1418.

Davis A. M. 1985. Refractory inclusions in the Ornans CO3 chondrite (abstract). 16th Lunar and Planetary Science Conference. pp. 165–166.

Davis A. M. and Hinton R. W. 1986. Magnesium and titanium isotopic compositions and trace element chemistry of refractory inclusions in the Ornans carbonaceous chondrite (abstract). 17th Lunar and Planetary Science Conference. pp. 154–155.

Davis A. M., Simon S. B., and Grossman L. 1994. Alteration of Allende type B1 CAIs: When, where and how (abstract). 25th Lunar and Planetary Science Conference. pp. 315–316.

Fagan T. J., Krot A. N., and Keil K. et al. 2000. Calcium-aluminum-rich inclusions in enstatite chondrites (I): Mineralogy and textures. *Meteoritics & Planetary Science* 35:771–781.

Fagan T. J., McKeegan K. D., Krot A. N., and Klaus K. 2001. Calcium-aluminum-rich inclusions in enstatite chondrites (II): Oxygen isotopes. *Meteoritics & Planetary Science* 36:223–230.

Fagan T. J., Guan Y., and MacPherson G. J. 2007. Al-Mg isotopic evidence for episodic alteration of Ca-Al-rich inclusions from Allende. *Meteoritics & Planetary Science* 42:1221–1240.

Frost M. J. and Symes R. F. 1970. A zoned perovskite-bearing chondrule from the Lancé meteorite. *Mineralogical Magazine* 37:724–726.

Geiger T. and Bischoff A. 1995. Formation of opaque minerals in CK chondrites. *Planetary and Space Science* 43:485–498.

Grossman J. N. 1996. The Meteoritical Bulletin, No. 80. *Meteoritics & Planetary Science* 31:A175–A180.

Grossman J. N. 1998. The Meteoritical Bulletin, No. 82. *Meteoritics & Planetary Science* 33:A221–A239.

Grossman J. N. 1999. The Meteoritical Bulletin, No. 83. *Meteoritics & Planetary Science* 34:A169–A186.

Grossman J. N. 2000. The Meteoritical Bulletin, No. 84. *Meteoritics & Planetary Science* 35:A199–A225.

Grossman J. N. and Zipfel J. 2001. The Meteoritical Bulletin, No. 85, *Meteoritics & Planetary Science* 36:A293–A322.

Grossman J. N., Rubin A. E., and MacPherson G. J. 1988. Allan Hills 85085: A unique volatile-poor carbonaceous chondrite with implications for nebular agglomeration and fractionation processes. *Earth and Planetary Science Letters* 91:33–54.

Grossman L. 1980. Refractory inclusions in the Allende meteorite. *Annual Review of Earth and Planetary Sciences* 8:559–608.

Grossman L. and Ganapathy R. 1975. Volatile elements in Allende inclusions. Proceedings, 6th Lunar Science Conference. pp. 1729–1736.

Grossman L. and Ganapathy R. 1976. Trace elements in Allende meteorite-II. Fine-grained Ca-rich inclusions. *Geochimica et Cosmochimica Acta* 40:149–155.

Grossman L., Fruland R. M., and Mckay D. S. 1975. Scanning electron microscopy of a pink inclusion from the Allende meteorite. *Geophysical Research Letters* 2:37–40.

Guan Y., Huss G. R., MacPherson G. J., and Wasserburg G. J. 2000a. Calcium-aluminum-rich inclusions from enstatite chondrites: Indigenous or foreign? *Science* 289:1330–1333.

Guan Y., McKeegan K. D., and MacPherson G. J. 2000b. Oxygen isotopes in calcium-aluminum-rich inclusions from enstatite chondrites: New evidence for a single CAI source in the solar nebula. *Earth and Planetary Science Letters* 181:271–277.

Guan Y., Huss G. R., MacPherson G. J., and Leshin L. A. 2002. Aluminum-magnesium isotopic systematics of aluminum-rich chondrules in unequilibrated enstatite chondrites (abstract #2034). 33rd Lunar and Planetary Science Conference. CD-ROM.

Hashimoto A. and Grossman L. 1985. SEM-petrography of Allende fine-grained inclusions (abstract). 16th Lunar and Planetary Science Conference. pp. 323–324.

Huss G. R., Wasserburg G. J., Russell S. S., and MacPherson G. J. 1997. Trace-element abundances and the origin of aluminum-26-bearing chondrules in unequilibrated ordinary chondrites (abstract). *Meteoritics & Planetary Science* 32:A63.

Huss G. R., MacPherson G. J., Wasserburg G. J., Russell S. S., and Srinivasan G. 2001. Aluminum-26 in calcium-aluminum-rich inclusions and chondrules from unequilibrated ordinary chondrites. *Meteoritics & Planetary Science* 36:975–997.

Ihinger P. D. and Stolper E. 1986. The color of meteoritic hibonite: An indicator of oxygen fugacity. *Earth and Planetary Science Letters* 78:67–79.

Ireland T. R. 1988. Correlated morphological, chemical and isotopic characteristics of hibonites from the Murchison carbonaceous chondrite. *Geochimica et Cosmochimica Acta* 52:2827–2839.

Ireland T. R., Zinner E. K., Fahey A. J., and Esat T. M. 1991. Hibonite-bearing microspherules: A new type of refractory inclusion with large isotopic anomalies. *Geochimica et Cosmochimica Acta* 55: 367–379.

Ivanova M. A., Pataev M. I., MacPherson G. J., Nazarov M. A., Taylor L. A., and Wood J. A. 2002. The first known natural occurrence of $CaAl_2O_4$, in a Ca-Al-rich inclusion from the CH chondrite NWA 470. *Meteoritics and Planetary Science* 37: 1337–1344.

Jäckel A., Bischoff A., Clayton R. N., and Mayeda T. K. 1996. Dar al Gani 013—A new Saharan Rumuruti chondrite (R3-6) with highly unequilibrated (type 3) fragments (abstract). 27th Lunar and Planetary Science Conference. pp. 595–596.

Kallemeyn G. W., Rubin A. E., and Wasson J. T. 1996. The compositional classification of chondrites: VII. The R chondrite group. *Geochimica et Cosmochimica Acta* 60:2243–2256.

Kimura M., El Goresy A., Palme H., and Zinner E. 1993. Ca-Al-rich inclusions in the unique chondrite ALH 85085: Petrology, chemistry and isotopic compositions. *Geochimica et Cosmochimica Acta* 57: 2329–2359.

Kimura M., Hiyagon H., Palme H., Spettel B., Wolf D., Clayton R. N., Mayeda T. K., Sato T., Suzuki A., and Kojima H. 2002. Yamato-792947, 793408, and 82038: The most primitive H chondrites, with abundant refractory inclusions. *Meteoritics & Planetary Science* 37:1417–1434.

Kornacki A. S. and Wood J. A. 1984. Petrography and classification of Ca,Al-rich and olivine-rich inclusions in the Allende CV3 chondrite. *Journal of Geophysical Research* 89:B573–B587.

Kornacki A. S. and Wood J. A. 1985. The identification of Group II inclusions in carbonaceous chondrites by electron microprobe analysis of perovskite. *Earth Planetary Science Lett*ers 72:74–86.

Kornacki A. S., Cohen R. E., and Wood J. A. 1983. Petrography and classification of refractory inclusions in the Allende and Mokoia CV3 chondrites. *Memoirs of the NIPR Symposium on Antarctic Meteorites, Special Issue* 30:45–60.

Krot A. N., Hutcheon I. D., and Keil K. 2002. Plagioclase-rich chondrules in the reduced CV chondrites: Evidence for complex formation history and genetic links between calcium-aluminum-rich inclusions and ferromagnesian chondrules. *Meteoritics & Planetary Science* 37:155–182.

Krot A. N., Scott E. R. D., and Zolensky M. E. 1995. Mineralogical and chemical modification of components in CV3 chondrites: Nebular or asteroidal processing. *Meteoritics* 30:748–776.

Krot A. N., Fagan T. J., Keil K., McKeegan K. D., Sahijpal S., Hutcheon I. D., Petaev M. I., and Yurimoto H. 2004. Ca,Al-rich inclusions, amoeboid olivine aggregates, and Al-rich chondrules from the unique carbonaceous chondrite Acfer 094: I. Mineralogy and petrology. *Geochimica et Cosmochimica Acta* 68:1873–1881.

Kurat G. 1975. Der kohlige Chondrit Lancé: Eine petrologische analyses der komplexen genese eines chondriten. *Tschermaks Mineralogische und Petrographische Mitteilungen* 22:38–78.

Lin Y., Guan Y., Leshin L. A., Ouyang Z., and Wang D. 2005. Short-lived chlorine-36 in a Ca- and Al-rich inclusion from the Ningqiang carbonaceous chondrite. *Proceedings of the National Academy of Sciences* 102:1306–1311.

MacPherson G. J. 2003. Calcium-aluminum-rich inclusions in chondritic meteorites. In *Meteorites, comets, and planets*, edited by Davis A. M. Treatise on Geochemistry, vol. 1. Oxford: Elsevier-Pergamon. pp. 201–246.

MacPherson G. J. and Davis A. M. 1994. Refractory inclusions in the prototypical CM chondrite, Mighei. *Geochimica et Cosmochimica Acta* 58:5599–5625.

MacPherson G. J. and Delaney J. S. 1985. A fassaite-two olivine-pleonaste-bearing refractory inclusion from Karoonda. 16th Lunar and Planetary Science Conference. pp. 515–516.

MacPherson G. J. and Grossman L. 1979. Melted and non-melted coarse-grained Ca-, Al-rich inclusions in Allende. *Meteoritics* 14:479.

MacPherson G. J. and Huss G. R. 2000. Convergent evolution of CAIs and chondrules: Evidence from bulk compositions and a cosmochemical phase diagram (abstract #1838). 31st Lunar and Planetary Science Conference. CD-ROM.

MacPherson G. J. and Huss G. R. 2005. Petrogenesis of Al-rich chondrules: Evidence from bulk compositions and phase equilibria. *Geochimica et Cosmochimica Acta* 69:3099–3127.

MacPherson G. J., Grossman L., Allen J. M., and Beckett J. R. 1981. Origin of rims on coarse-grained inclusions in the Allende meteorite. Proceedings, 12th Lunar and Planetary Science Conference. pp. 1079–1091.

MacPherson G. J., Bar-Matthews M., Tanaka T., Olsen E., and Grossman L. 1983. Refractory inclusions in the Murchison meteorite. *Geochimica et Cosmochimica Acta* 47:823–839.

MacPherson G. J., Grossman L., Hashimoto A., Bar-Matthews M., and Tanaka T. 1984. Petrographic studies of refractory inclusions

from the Murchison meteorite. Proceedings, 15th Lunar and Planetary Science Conference. pp. C299–C312.

MacPherson G. J., Wark D. A., and Armstrong J. T. 1988. Primitive materials surviving in chondrites: Refractory inclusions. In *Meteoritics and the early solar system*, edited by Kerridge J. F. and Matthews M. S. Tucson, Arizona: The University of Arizona Press. pp. 746–807.

McGuire A. V. and Hashimoto A. 1989. Origin of zoned fine-grained inclusions in the Allende meteorite. *Geochimica et Cosmochimica Acta* 53:1123–1133.

Methot R. L., Noonan A. F., Jarosewich E., de Gasparis A. A., and Al-Far D. M. 1975. Mineralogy, petrology and chemistry of the Isna (C3) meteorite. *Meteoritics* 10:121–131.

Morimoto N., Fabries J., Ferguson A. K., Ginjburg I. V., Ross M., Seifert F. A., Zussman J., Aoki K., and Gottardi G. 1988. Nomenclature of pyroxenes. *American Mineralogist* 73:1123–1133.

Noguchi T. 1993. Petrology and mineralogy of CK chondrites: Implications for metamorphism of the CK chondrite parent body. *Proceedings of the NIPR Symposium on Antarctic Meteorites* 6: 204–233.

Rout S. S. and Bischoff A. 2007. CAIs in Rumuruti chondrites (abstract). *Geochimica et Cosmochimica Acta* 71:A855.

Rubin A. E. and Kallemeyn G. W. 1989. Carlisle Lakes and Allan Hills 85151: Members of a new chondrite grouplet. *Geochimica et Cosmochimica Acta* 53:3035–3044.

Rubin A. E. and Kallemeyn G. W. 1994. Pecora Escarpment 91002: A member of the new Rumuruti (R) chondrite group. *Meteoritics* 29:255–264.

Russell S. S. 1998. A Survey of calcium-aluminum-rich inclusions from Rumurutiite chondrites: Implication for relationship between meteorite groups (abstract). *Meteoritics & Planetary Science* 33:A131–A132.

Russell S. S., Leshin L. A., McKeegan K. D., and MacPherson G. J. 1997. Oxygen isotope composition of aluminum-rich chondrules: Clues to their origins (abstract). *Meteoritics & Planetary Science* 32:A111.

Russell S. S., Huss G. R., Fahey A. J., Greenwood R. C., Hutchison R., and Wasserburg G. J., 1998a. An isotopic and petrologic study of calcium-aluminum-rich inclusions from CO3 meteorites. *Geochimica et Cosmochimica Acta* 62:689–714.

Russell S. S., Leshin L. A., McKeegan K. D., and MacPherson G. J. 1998b. Oxygen-16 enrichment in aluminum-rich chondrules from unequilibrated ordinary chondrites (abstract). 29th Lunar and Planetary Science Conference. pp. 1826–1826.

Russell S. S., Davis A. M., MacPherson G. J., Guan Y., and Huss G. R. 2000a. Refractory inclusions from the ungrouped carbonaceous chondrites MAC 87300 and MAC 88107. *Meteoritics & Planetary Science* 35:1051–1066.

Russell S. S., MacPherson G. J., Leshin L. A., and McKeegan K. D. 2000b. ^{16}O enrichments in aluminum-rich chondrules from ordinary chondrites. *Earth and Planetary Science Letters* 184: 57–74.

Russell S. S., Zipfel J., Folco L., Jones R., Grady M. M., McCoy T., and Grossman J. N. 2003. The Meteoritical Bulletin, No. 87. *Meteoritics & Planetary Science* 38:A189–A248.

Russell S. S., Zolensky M., Righter K., Folco L., Jones R., Connolly Jr. H. C., Grady M. M., and Grossman J. N. 2005. The Meteoritical Bulletin, No. 89. *Meteoritics & Planetary Science* 40:A201–A263.

Schulze H. and Otto J. 1993. Rumuruti: A new Carlisle Lakes-type chondrite (abstract). *Meteoritics* 28:433.

Schulze H., Bischoff A., Palme H., Spettel B., Dreibus G., and Otto J. 1994. Mineralogy and chemistry of Rumuruti: The first meteorite fall of the new R-chondrite group. *Meteoritics* 29:275–286.

Sheng Y. J., Hutcheon I. D., and Wasserburg G. J. 1991. Origin of plagioclase-olivine inclusions in carbonaceous chondrites. *Geochimica et Cosmochimica Acta* 55:581–599.

Simon S. B., Grossman L., and Davis A. M. 1991. Fassaite composition trends during crystallization of Allende Type B refractory inclusion melts. *Geochimica et Cosmochimica Acta* 55:2635–2655.

Simon S. B., Yoneda S., Grossman L., and Davis A. M. 1994. A $CaAl_4O_7$-bearing refractory spherule from Murchison: Evidence for very high-temperature melting in the solar nebula. *Geochimica et Cosmochimica Acta* 58:1937–1949.

Simon S. B., Davis A. M., Grossman L., and Zinner E. K. 1998. Origin of hibonite-pyroxene spherules found in carbonaceous chondrites. *Meteoritics & Planetary Science* 33:411–424.

Srinivasan G., Huss G. R., and Wasserburg G. J. 2000. A petrographic, chemical and isotopic study of calcium-aluminum-rich inclusions and aluminum-rich chondrules from the Axtell (CV3) chondrite. *Meteoritics & Planetary Science* 35:1333–1354.

Tomeoka K., Nomura K., and Takeda H. 1992. Na-bearing Ca-Al-rich inclusions in the Yamato-791717 CO carbonaceous chondrite. *Meteoritics* 27:136–143.

Tronche E. J., Hewins R. H., and MacPherson G. J. 2007. Formation conditions of aluminum-rich chondrules. *Geochimica et Cosmochimica Acta* 71:3361–3381.

Ushikubo T., Guan Y., Hiyagon H., Sugiura N., and Leshin L. 2007. ^{36}Cl, ^{26}Al and O isotopes in an Allende type B2 CAI: Implication for multiple secondary alteration events in the early solar system. *Meteoritics & Planetary Science* 42:1267–1279.

Wark D. A. 1979. Birth of the presolar nebula: The sequence of condensation revealed in the Allende meteorite. *Astrophysics and Space Science* 65:275–295.

Wark D. A. 1981. Alteration and metasomatism of Allende Ca-Al-rich materials (abstract). 12th Lunar and Planetary Science Conference. pp. 1145–1147.

Wark D. A. and Lovering J. F. 1977. Marker events in the early evolution of the solar system: Evidence from rims on Ca-Al-rich inclusions in carbonaceous chondrites. Proceedings, 8th Lunar Science Conference. pp. 95–112.

Weber D. and Bischoff A. 1994. The occurrence of grossite ($CaAl_4O_7$) in chondrites. *Geochimica et Cosmochimica Acta* 58: 3855–3877.

Weber D. and Bischoff A. 1997. Refractory inclusions in the CR chondrite Acfer 050-El Djouf 001: Petrology, chemical composition, and relationship to inclusion populations in other types of carbonaceous chondrites. *Chemie der Erde* 57:1–24.

Weber D., Zinner E., and Bischoff A. 1995. Trace element abundances and Mg, Ca, and Ti isotopic compositions of grossite-containing inclusions from the carbonaceous chondrite Acfer 182. *Geochimica et Cosmochimica Acta* 59:803–823.

Weber D., Schultz L., Weber H. W., Clayton R. N., Mayeda T. K., and Bischoff A. 1997. Hammadah al Hamra 119—A new, unbrecciated Saharan Rumuruti chondrite (abstract). 28th Lunar and Planetary Science Conference. pp. 1511–1512.

Weber H. W. and Schultz L. 1995. Noble gases in Rumuruti-group chondrites (abstract). *Meteoritics* 30:596.

Weisberg M. K., Prinz M., Kojima H., Yanai K., Clayton R. N., and Mayeda T. K. 1991. The Carlisle Lakes-type chondrites: A new grouplet with high $\Delta^{17}O$ and evidence for nebular oxidation. *Geochimica et Cosmochimica Acta* 55:2657–2669.